THE EFFECT OF THE DUST PARTICLE SIZE ON DUST EXPLOSIONS

Thesis by

Champlain Landry

Department of Mechanical Engineering

McGill University

Montreal, Quebec, Canada

Submitted June 1994

A Thesis submitted to the Faculty of Graduate Studies
and Research in partial fulfillment of the
requirements of the degree of Master's of Engineering

Abstract

The study of dust combustion is of fundamental importance in determining the explosive characteristics of given dust suspensions. Researchers have studied how parameters such as concentration of dust, ignition energy, etc., influence dust combustion. However, the effect of the dust particle size has not been systematically investigated. In particular researchers do not distinguish between the inability of larger dust particle's to be dispersed and the slower burning rates associated with larger dust particles.

Results from this study show that for small dust particles the experimental conditions in which the experiments are performed have little effect on the results. On the other hand, when larger dust particles are used, the effects of settling are quite significant, explaining the reduction in maximum overpressure compared to smaller dust. Furthermore, it was observed that the settling of large particles is not only due to gravity. In fact, removal of dust due to swirling of the suspension accounts for a significant reduction in dust concentration.

Résumé

L'étude de la combustion de particules est d'une importance fondamentale dans la détermination des paramètres d'explosion d'une suspension de particules. Les chercheurs ont étudié l'effet qu'avaient les paramètres tels que la concentration de poussière, l'énergie d'allumage, etc., sur la combustion de poussière. Mais l'étude de l'influence de la dimension des particules n'a pas été faite de façon systématique. En particulier, les chercheurs ne distinguent pas entre l'incapacité de créer une suspension et la diminution de rythme d'augmentation de pression associé avec des dimensions de particule plus grande.

Les résultats démontrent pour de fines particules que la condition dans laquelle les expériences sont conduites influence peu les résultats. D'un autre côté, lorsque les expériences sont conduites avec des particules plus grosses, l'effet de déposition des particules est significatif, expliquant la réduction en surpression maximale d'explosion. De plus, il a été observé que la déposition de particules ne serait pas entièrement due à la gravité. En effet il y a diminution de concentration des particules; celles-ci collent à la parois de la chambre de combustion due à la vorticité de la suspension.

Acknowledgments

The first person I must acknowledge is my supervisor: Professor John H. S. Lee. He is the person that inspired me as a young under grade to pursue graduate studies. He taught me to always demand more out of myself and to be a better student for it. For these reasons I am greatly in debt to him. Even though he is an extremely busy man and a very active personality in the international research community, he always had time to read what I had done or to discuss the problems that I was faced with.

Special thanks must go to Dr Olivier Peraldi, with who I spent a great amount of time in my last year as an under grade and my first year as a grad-student, working in the lab. Olivier showed me how to overcome technical difficulties related to experimental work and he was the first to introduce me to the basic concepts of dust combustion while at the same time being a good friend.

I also acknowledge the help and inspiration of Dr Samuel Goroshin. A researcher with many years of very rich experience in the field of dust explosions. Being of the former Soviet Union, Dr Goroshin exposed me to previously unavailable scientific knowledge and also a very rich cultural heritage.

I would like to thank Dr Aris Makris, for the constant encouragement that he gave me during the period of thesis preparation. His help was very dear to me, considering he had just been through the process of completing his Ph.D. thesis, he could relate to what I was going through.

I would also like to thank Kathleen Sawler, Prof. Lee's secretary. She was extremely helpful in keeping the communication lines open with Prof. Lee even when he was half way around the world. Thank you also for the great help in the thesis preparation.

I would like to thank Michele Shemie for helping me make this thesis not sound too much as if it was written by a *Francophone* and for all the discussions that we had. I would also like to thank Kosta Kannelis and

Nick Konidas for their help in putting together the visualization experiment.

I would like to acknowledge Tom Scarinci and Denis Palin for their help in making the final correction to the thesis.

Finally I would like to acknowledge members of my family, my girlfriend Eve and Sammy jr. for their constant support and understanding during the preparation of this work.

This work was supported by the Canadian Space Agency, under contract 9F007-2-6026/01-SW.

Table of Contents

List of Notations

Al	-Aluminum
d	-Diameter
d_{32}	-Sauter Mean Diameter
dP/dt	-Pressure Rise Rate
F	-Force
Kst	-Normalized Pressure Rise Rate
n	-Number of Moles of Gas
N_2	-Nitrogen
O_2	-Oxygen
P	-Pressure
R	-Radius
S	-Burning Velocity
S_f	-Flame Speed
t	-Time
T	-Temperature
V	-Volume
Δ	-Finite Change from Initial to Present
γ	-Specific Heat Ratio
ρ	Density
$\mathfrak{R}$	-Specific Gas Constant

suspension [9,10,11,12,13], affects the violence of the explosive events in terms of peak pressure and also the maximum rate of pressure rise.

Numerous researchers have studied how the maximum pressure and the maximum rate of pressure rise are affected by the size of the dust particles. Results show that as the size of the particles increases the maximum pressure and the maximum rate of pressure rise decrease [14,15,16]. However, the mechanisms of how dust particle size affects the maximum pressure and the maximum rate of pressure rise have not been studied. In particular, results obtained do not distinguish between the inability of the dispersion systems used to create a uniform suspension or the reduction of burning rates associated with larger particle sizes.

The size of the dust particles affects the combustion characteristics of a dust cloud by modifying the surface area to volume ratio of the individual particles. As the size of the dust particles increases, the specific surface area of the dust sample decreases which means the area over which burning can occur is reduced [15]. Consequently, the rate of heat release in a dust explosion decreases as the size of the dust particles increases.

The size of the dust particles also affects the ability of dust to stay in suspension. In experimental chambers, dust suspensions are generated by using air jets that lift the dust and then create mixing to render the suspension uniform. Once the dispersion process is completed, the dust is subjected to external forces, such as gravity that will tend to settle the dust. As the dust particles move through the air, the resistance of the air will oppose the motion. Thus the balance of drag and gravitational force exerted on dust particles is what governs the settling velocity of the particles [17]. According to Stoke's viscous flow theory [17], the drag force is proportional to the diameter of the particle, while the gravitational force is proportional to the mass of the particle or the volume of the particle multiplied by its density. This means that the ratio of gravitational force to drag force is proportional to the square diameter of the particle, i.e. $[F_{gravitational}/F_{drag}] \alpha d^2$. Therefore, as the size of the particles increases, the gravitational force dominates, and the particles tend to settle faster. Fallen particles cannot participate in the combustion process therefore reducing the total amount of energy released as well as the rate at which it is released.

In conclusion, this implies that the combined effect of the change in distribution of the dust in the combustion chamber and the modification of the burning rate result in a strong influence of dust particles size on the explosion characteristics, being the maximum overpressure and the maximum rate of pressure rise.

Because previous experimental work has not yet determined the relative importance of settling of dust and the change in burning characteristics associated with different particle sizes, a systematic investigation needs to be undertaken to establish clearly the role of the dust particle size. Hence the aim of this investigation will be to attempt to separate the effect of dust depletion of the suspension from the change in burning rate associated with the change in particle size.

In order to accomplish this task, different experimental conditions will be required. Different types of dispersion systems will be used in order to observe the burning of suspensions of various turbulent intensities. The size of the dust particles tested will be changed in order to study the different rates of settling associated with each of the characteristic sizes of dust. Finally the size of the combustion chamber in which the experiments are performed will be changed in order to establish the effect of the scale of the dispersion turbulence on the rate of settling of the dust particles in the suspension.

As gravity settling occurs, the concentration of dust in the suspension decreases and therefore the experimental conditions are changed. For this reason, it is necessary to perform experiments in a reduced gravity environment in order to reduce settling effects [18]. Microgravity offers a unique non settling environment in which dust combustion experiments can be performed with greater certainty [19,20,21]. As well as providing a non settling environment, microgravity offers a non buoyant environment. Buoyancy forces tend to inhibit the propagation of slow flames by heavily perturbing the flame front [22,23]. A series of tests involving different dust particles' diameters will be performed in reduced gravity conditions in order to establish the effect of gravitational settling. The reduced gravity experiments performed for this investigation were done aboard the NASA KC-135 parabolic trajectory plane [24].

In addition to the results obtained in the various combustion chambers, a photographic investigation of the dispersion process was also performed. The aim of these visualization experiments was to characterize the time evolution of the suspension in terms of uniformity and concentration of the dust cloud. This was done for various sizes of dust particles to see how this would affect the development of the suspension.

2-Experimental Description

2.1-Introduction

A description of the experimental conditions in which the tests were performed is hereby presented. This will include the description of the different experimental hardware, the dusts used in the tests as well as the experimental procedure.

2.2-Combustion Experiments

The combustion experiments performed in this investigation were done under constant volume conditions. These types of experiments are preferred because by simply monitoring the pressure evolution of the combustion process, information on the amount of energy and on the global rate of the energy released can be derived.

Four experimental apparatus were used to perform this series of tests. The apparatus varied either by the dispersion system used to generate the dust suspension or by the volume of the combustion chambers. All the types of dispersion systems used in this investigation relied on turbulent air jets to disperse the dust in the chamber. The different experimental chambers shared a common control panel that permitted the control of the initial pressure in the combustion chamber and the pressure in the high pressure storage vessel for the dispersion air, the same ignition control and the same data acquisition system. Figure 1 shows the typical layout of the experimental apparatus with the control panel.

A more detailed description of each of the different combustion chambers and the type of dispersion system used follows.

2.2.1-Ground Based Experimental Apparatus

2.2.1.1-The 4.4 Liter Sphere with Hartmann [25] Type Dispersion System.

The combustion chamber is a 4.4 liter stainless steel sphere, composed of two hemispheres joined together using a bolted flange. A small hemispherical shell, used to disperse the dust, is placed at the bottom of the chamber. A tube is directed at the center of the hemispherical shell from which a strong air jet comes out and impacts the dust that had previously been placed in the hemispherical cup. Figure 2 shows the configuration of the sphere with the dispersion system. The air jet lifts the dust as it is deflected by the hemispherical cup and turbulent mixing distributes the dust in the combustion chamber.

The dispersion tube is connected to a high pressure dispersion chamber. A solenoid valve is used to control the flow from the high pressure vessel to the dispersion tube.

2.2.1.2-The 4.4 Liter Chamber with Dispersion Ring

This experimental chamber is similar to the 20 liter sphere used by the Bartknecht group [1,7]. The combustion chamber is essentially the same stainless steel sphere described in the previous section, except that it has been fitted with a dispersion ring instead of the Hartmann type dispersion system. The dispersion ring is connected to an external dust cup. Figure 3 describes the chamber and the dust cup assembly. Figure 4 shows a detailed view of the dust cup.

The deagglomeration of the dust sample, via strong air jets, occurs in the external dust cup. Once the dust sample has been broken up, the suspension flows in the dispersion ring where it is distributed into the combustion chamber. The ring is made of a copper tube that has an inner diameter of 0.6 cm. The ring itself has a diameter of 20 cm and has 30 holes of 1 millimeter in diameter directed radially inward.

The external dust cup is connected to the high pressure vessel separated by a solenoid valve. The dispersion is controlled by the solenoid valve placed between the external dust cup and the high pressure dispersion vessel.

2.2.1.3-The 5.4 Liter Sphere with Conical Diffuser.

This dispersion system, developed at McGill University [26], uses an external dust cup to deagglomerate the dust and a conical diffuser, located inside the combustion chamber, to distribute the dust in the combustion chamber. Figure 5 shows a diagram of the sphere and the dispersion system. Figure 6 shows a detailed view of the dust cup and the diffuser cone assembly. The combustion chamber is a 5.4 liter copper, composed of two hemispheres joined together by a bolted flange. As in the case of the dispersion ring system, the suspension is created in the external dust cup. The suspension then flows through a constant area duct to reduce the suspension's turbulent intensity. The suspension is then dispersed in the combustion chamber through the conical diffuser.

The external dust cup is connected to a high pressure storage chamber. The flow of air is controlled by a solenoid valve placed between the dust cup and the high pressure storage chamber.

2.2.1.4-The 35 Liter Cylinder with Hartmann [25] Dispersion System.

The 35 liter vessel has a cylindrical geometry. Figure 7 shows the combustion chamber with the dispersion system at the bottom of the chamber. It has a length to diameter ratio of 1.2:1. Similar in design to the 4.4 liter sphere, also consisting of the Hartmann type dispersion system, a hemispherical cup is placed at the bottom of the chamber. A tube is directed at the middle of the hemispherical cup in order to disperse the dust.

The dispersion tube is connected to a high pressure storage vessel. The high pressure chamber of this particular system is larger than the three previous ones, because the volume of the combustion chamber is much larger. Therefore the dispersion jets must be stronger in order to attain a uniform distribution of dust in the chamber. The dispersion process is controlled by a solenoid valve placed between the high pressure storage vessel and the dispersion tube.

2.2.2-Microgravity Experimental Set-Up

2.2.2.1-Description

The experiments performed in microgravity used the same combustion chamber as described in the 5.4 liter sphere equipped with a conical diffuser dispersion system. For the microgravity performed experiments the experimental apparatus was mounted in a rack that will be described later in the text.

The microgravity experiments were performed aboard the NASA KC-135. During each flight, the plane performs 40 parabolas, during which there is approximately 20 seconds of reduced gravity ($\approx 10^{-2}$ g). Because the experiments were performed in a plane, it is vital that all the necessary components be included in the experimental rack. To carry out the experiments on board the NASA KC-135 aircraft, a self-contained system comprising a vacuum system, compressed air and data acquisition system was developed. A schematic illustration of the microgravity laboratory is shown on Figure 8.

It should be noted that the experimental apparatus used in the microgravity plane is identical to the one used for ground-based experiments. This is important in order to be able to compare data in the two different conditions.

2.2.3-Ignition system

The ignition system used in all the combustion experiments was a pyrotechnic ignitor. This ignitor is in the form of an electric match. A charge of gun powder is distributed on a glow wire. To initiate the ignitor, a small current is passed through the glow wire, heating it up and igniting to the gun powder.

This type of ignitor was chosen for its reproducible ignitions. The energy yield is sufficient to ignite all of the different mixtures tested but at the same time, small enough so that it does not noticeably affect the final maximum overpressure in the combustion chamber. Tests have been performed, using only an electric match ignitor in the combustion chamber and monitoring the pressure inside the chamber in order to determine whether there is a pressure rise. All the tests performed show an indiscernible pressure rise from the ignitor alone.

The ignitor, in all the experimental configurations, was placed in the middle of the chamber at the end of a holding electrode, as it is shown in Figure 2, 3, 5 and 7.

2.2.4-Data Acquisition

The data acquisition system is a computer fitted with an oscilloscope card. The sampling rate of data was 1 MHz. This rate is sufficient since the process that it is monitoring is of the order of millisecond, as can be seen later.

In order to record the pressure time history of the combustion process, the combustion chamber had to be fitted with pressure transducers. The transducers used a piezoelectric crystal with a stainless steel diaphragm [PCB 113A24, 5 mV/psi, or 73.5 mV/bar]. The pressure transducer had to be covered with heat shields to protect it from the intense heat of the flame. Without the heat shield, the diaphragm would have become distorted due to thermal expansion and the pressure signal would have been corrupted.

2.2.5-Test Procedure for the Combustion Experiments

The procedures for all the apparatus used are kept uniform in order to have the most analogous results possible. The first step is to place the pyrotechnic ignitor on the holding electrode. The dust sample that is to be tested is placed in the appropriate dispersion system. The combustion chamber is then closed and completely vacuumed in order to eliminate all of the impurities and humidity that can be found in atmospheric air. The combustion chamber is then filled with extra dry air to a given sub atmospheric pressure. The reason why the combustion chamber is not filled to atmospheric pressure is that the dispersion process uses air jets that add air in the sealed combustion chamber. If the combustion chamber were to be initially filled to atmospheric pressure, the pressure after the dispersion process would be higher than atmospheric pressure due to the additional air of the dispersion jets.

The high pressure dispersion chamber is pressurized to its assigned pressure. It should be noted that the ratio of the dispersion pressure and the pressure at which the combustion chamber is filled needs to be calculated in order to insure that the final pressure, after dispersion, in the combustion chamber is one atmosphere. See Appendix A for the calculation of the partially filled pressure with respect to the dispersion pressure.

Once the combustion chamber is ready for the ignition, the electronic control of the system has to be prepared. The test procedure has a certain sequence in which events must occur. Prior to ignition the dispersion process must be completed. This means that there must be a delay between the dispersion sequence and the ignition. This is the function of the electronic control system. In the combustion test procedure, there are two distinct events: the dispersion sequence and the ignition. The dispersion is the first phase to occur. In this phase the solenoid valve that controls the dispersion process is activated and the dispersion air in the high pressure chamber starts dispersing the dust. Simultaneously to this, an electronic pulse is sent to a delay generator that has been preset to allow for enough time for the dispersion process to occur. Once the delay period has expired, the delay generator sends a second electronic pulse to the ignition control switch and ignition of the suspension occurs. At the same time a pulse is sent to the data acquisition system to begin the recording of the pressure time history profile of the combustion process. Note that for each experimental apparatus the delay before ignition is varied in order to determine the optimal conditions of dispersion.

Once the combustion process is completed, the recorded data is stored and the sphere is opened and cleaned of the combustion products. The sphere is now ready for another trial.

2.3-Dispersion Visualization Experiments

2.3.1-Description of Experimental Apparatus

In order to be able to visualize and study the dispersion process of dust, the vessel in which the dispersion is performed must be transparent. A simple solution to this problem is to perform the dispersion in an inflated transparent balloon. The balloon can be inflated to the desired volume and the dispersion system can be fitted at the opening of the balloon. The walls of the balloon are rigid enough to contain the dispersion process in such a way that the dispersion process is quite similar to what occurs in a rigid sphere.

The dispersion system used is similar to the diffuser cone with an external dust cup used in the combustion experiments. There are slight differences in the design of the dust cup and the diffuser cone, but the general design remains the same.

The balloon and dispersion system assembly are contained in a larger vessel that would hold the suspension in case of an accidental burst of the balloon. This containment also protects the operator in case of an accidental ignition of the suspension in the balloon. A schematic of the assembly of the dispersion system and the balloon can be seen in Figure 9. The balloon and the containment vessel can be seen in Figure 10.

2.3.2-Test Procedure for the Visualization Experiments

The experimental procedure of the visualization experiments is quite similar to those of the combustion experiments except for the fact that the suspension is not ignited. Additional steps such as the inflation of the balloon and the initialization of the video camera had to be performed prior to each shot. Other than these the two steps, the visualization experiments were similar to the combustion experiments.

In order to have a permanent record of the dispersion process, it was necessary to film the dispersion. In this case, a standard VHS video camera was used to record the dispersion process. The video camera was activated prior to the dispersion process. Once the dispersion has occurred and the whole process has been recorded, the video camera is simply turned off.

At this point, the containment vessel is cleaned of all the dust, a new balloon is placed on the balloon holder, and the apparatus is ready for the next trial.

2.4-Characteristics of the Dust

Any dust sample contains a wide variety of particle sizes. For this reason, it is difficult to determine a characteristic dimension for the dust particles. In order to describe the dimension of the particles in the dust sample, it is necessary to use an average diameter to characterize the typical dimension of the dust sample. This way, the dust sample can be described in one characteristic dimension.

There are different ways to describe the average size of the particles in a dust sample. These methods vary by the criteria used in determining the average size of the dust sample. The smallest diameter that represents 50 % of the dust sample by mass is defined as the median diameter. The median diameter can also be based on the diameter that represents half of the total number of particles. Depending on what parameter is desired, it is possible to define the average dimension using different methods.

The Sauter mean diameter d_{32} is often used to describe the average size of a dust sample [27]. The Sauter mean diameter is defined as:

$$d_{32} = \frac{n_i \sum_{i=1}^{n} d_i^3}{n_i \sum_{i=1}^{n} d_i^2} \qquad (2.1)$$

The Sauter diameter can be related to the average volume of the particles divided by the average surface area of the particles. It can be determined relatively easily by using a light scattering technique

The dust samples used in this investigation were all of the same chemical composition to allow comparison to be made between them. They were supplied by AMPAL of Flemington N-J. The chemical composition of the dust is 99.7% aluminum, 0.16% iron and 0.10 % silica (SiO_2). Three sizes of dust particles were used. The size of the particles used in this study have Sauter diameters' d_{32} as follows:

- dust 1: d_{32} = 5.4 μm
- dust 2: d_{32} = 18 μm
- dust 3: d_{32} = 40 μm

Prior to every test, the dust samples were dried in an oven for a period of at least 24 hours at a temperature of approximately 100 C. This insured that no traces of humidity were found in the dust sample that could cause agglomeration of the dust particles.

2.5-Concentration of Dust in the Suspension

In order to describe a dust suspension, it is necessary to specify the mass of dust that is present in the mixture. The concentration of a dust in a suspension is given by the number of grams of dust per cubic meter of air (g/m^3). In most experiments, the nominal concentration is used to describe the suspension in the combustion chamber. The nominal concentration is defined by the mass of dust put in the dispersion system, divided by the volume of the combustion chamber. The dispersion systems are not one hundred percent efficient, meaning that some fraction of the dust placed in the dispersion system does not get dispersed. The result being that the actual concentration of dust in the combustion chamber is less than the nominal concentration.

3-Results and Discussion

3.1-Constant Volume Combustion

The main source of information on the characteristics of the combustion process comes from the pressure time-history curve. A typical pressure time history curve is shown in Figure 11. The recorded overpressure, in bars, is on the y-axis and the x-axis represents the time evolution of the process.

The maximum explosion overpressure is related to the total chemical energy contained in the mixture. The overpressure inside the combustion chamber depends on what fraction of the dust has been burnt. The expression of the ideal pressure can be stated as follows:

$$\frac{P(t)}{P_{max}} = \frac{\text{Mass Burnt}}{\text{Mass Total}} = \frac{\frac{4}{3}\cdot\pi\cdot R^3_{flame}\rho_{Products}}{\frac{4}{3}\cdot\pi\cdot R^3_{sphere}\rho_{Reactants}} \qquad (3.1)$$

This can be reduced to:

$$\frac{P(t)}{P_{max}} = \frac{R^3_{flame}\rho_{Products}}{R^3_{sphere}\rho_{Reactants}} \qquad (3.2)$$

The density of products and reactants changes as the pressure in the combustion chamber increases, but the ratio of density remains unchanged and can be expressed as the constant C_1. Thus the expression can be further reduced to:

$$\frac{P(t)}{P_{max}} = \frac{R^3_{flame}}{R^3_{sphere}}\cdot C_1 \qquad (3.3)$$

The radius of the flame can be expressed as the flame speed (S_f) multiplied by the time of propagation. Thus the expression for pressure becomes:

$$\frac{P(t)}{P_{max}} = \frac{(S_f \cdot t)^3}{R^3_{sphere}} \cdot C_1 = C_2 \cdot t^3 \qquad (3.4)$$

Note that in the last part of this equation, S_f, R_{sphere} and C_1 have been combined into C_2 to simplify the expression. This expression clearly shows the dependence of pressure on the time evolution of the combustion process. Comparing this result with what is observed in Figure 11, it can be seen that for the initial stage of combustion the rise in pressure is low and increases rapidly with time. This is also the behavior of the cubic function that has been found.

If the derivative with respect to time of pressure versus time expression was taken the result would be:

$$\frac{dP(t)}{dt} = 3 \cdot P_{max} \cdot C_2 \cdot t^2 \qquad (3.5)$$

Thus, according to this last equation, the maximum rate of pressure rise (steepest slope) would occur at the end of the process (large t). However, from Figure 11 it can be seen that the maximum rate of pressure rise occurs before the maximum pressure is reached. The explanation for this phenomenon is that as the flame approaches the wall of the combustion chamber, heat losses become significant. Therefore the maximum rate of pressure rise occurs at some point where heat losses are not yet significant.

3.1.1-Comparison of Results with Published Data

In order to establish the validity of the present results, it is of interest to compare the data to already published results. Figure 12 shows the results of maximum explosion pressure of aluminum dust with varying dust concentration obtained by 4 investigators [1,9,28,29]. Added to this are results obtained in this investigation for a 4.4 liter sphere using 5.4μm dust particles.

It must be noted that in all the graphics included in this thesis, the curves to match the data points were drawn by hand using French curves. This was done in order to accommodate for the relatively large scatter of the data points.

It can be seen that the results obtained in this investigation are within the range of the results that have been obtained in the past. This indicates that the experimental conditions in which our results were obtained are comparable with conditions of other experimenters.

It can also be observed from Figure 12 that results obtained in combustion vessels of smaller volume tend to yield lower levels of maximum explosion pressure, as compared to experiments performed in larger vessels. The results obtained by Bartknecht [1] in the 1 m^3 (1000 liter) vessel and the results obtained by Pu [9] in the 20 liter vessel are significantly higher than the results obtained by Ishibana [29] in a 10 liter vessel or Jacobson [28] in the 1.2 liter vessel.

The main feature of this graph remains the large scatter that is observed from one author to another. This is caused by the difference in the experimental conditions in which each series of tests were performed. In fact, when experimental conditions are changed, the uniformity of the suspension or the amount of dust that will stick to the wall as well as the rate of dust sedimentation can change. The change of these conditions can results in significant differences in the maximum overpressure.

From Figure 12, it can also be seen that the maximum pressure increases as the concentration of dust in the suspension increases, until the concentration reaches 500 or 600 g/m^3. After this concentration, the maximum explosion pressure either remains constant or decreases slightly.

The stoichoimetry of the chemical reaction of aluminum in air is calculated in Appendix B. For stoichoimetric conditions, the concentration of dust is 310 g/m^3.

Since the maximum explosion pressure is found to occur when a suspension corresponds to approximately 600 g/m^3 of dust, this will be the optimal condition in which all other experiments will be performed. Note that this corresponds to an equivalence ratio of roughly 2.

3.1.2-Effects of Different Dispersion Method

In order to study the combustion of a dust sample, a suspension of the dust must be created. This is done by using some dispersion system that will break up the agglomeration of the dust and then disperse it inside the combustion chamber. The type of dispersion system used greatly influences how the dust will be distributed inside the combustion chamber.

3.1.2.1-Influence of Dispersion Intensity

In this study, the dispersions are achieved by using air jets that entrain the dust in the combustion chamber. By changing the configuration of the dispersion system, the flow of the dispersion air jets will change, modifying the distribution of the dust inside the combustion chamber.

In order to obtain a uniform distribution of dust in the vessel, the flow of the dispersion air must be quite turbulent, thus allowing sufficient mixing. The velocity of the flow as well as the average scale of the turbulent eddies that are created by the dispersion system will vary from one type of dispersion system to another.

Because the stream lines of the dispersion air will change from one type of dispersion system to another, the suspension that will be generated will also be different. For this reason, the uniformity of the suspension created is dependent on the type of dispersion system.

Another effect of the differences in flow fields is how the dust will follow the flow of the dispersion air. For air flow that has a high curvature and velocity, the dust particles will not be able to follow the stream lines of the dispersion air jets. This will lead to stratification of the suspension. Stratified suspensions tend to yield erratic results in maximum overpressure. Because the suspension has localized patches of high dust concentration, the dust patches may or may not participate in the combustion process and in some cases, the ignitor may be in a space that does not contain any dust, resulting in the non ignition of the suspension.

Another scenario of the particles being unable to follow the stream lines, is that the dust particles will completely separate from the dispersion air and impact the walls of the combustion chamber. After the dust particles have impacted the wall of the combustion chamber they tend to stick to the wall or become agglomerated with other particles. The result of these two effects will be less dust in the suspension.

As noted before, the maximum overpressure is proportional to the chemical energy present in the suspension [30]. Accordingly if there is a lot of aluminum dust in the suspension, the maximum overpressure will be high. If, on the other hand, there has been a lot of settling of dust and little dust remains in the suspension, the maximum overpressure will be lower than expected.

3.1.1.2-Results of Different Dispersion Systems

In order to illustrate the difference between types of dispersion systems, three different dispersion systems have been investigated. From the design of the different dispersion systems, it is expected that the flow field of the dispersion air in the combustion chamber will be quite different.

Figure 13 shows results of maximum overpressure for three types of dispersion systems with respect to ignition delay. A suspension of 600 g/m^3 of aluminum having a diameter of 5.4 μm was used.

This figure shows that for all three types of dispersion systems, the variation in maximum overpressure results is small. The reason being that small dust particles closely follow the dispersion air stream lines.

Therefore even if the dispersion flow has a high curvature, the dust suspension will not become as stratified and the dust will have less tendency to impact the wall and come out of suspension. The result being that most of the dust remains in suspension and The maximum overpressure is high.

Figure 13 shows a low decrease in overpressure with increasing delay between dispersion and ignition. This indicates that the rate of settling of the dust particles is low. Even after one second of ignition delay, the level of maximum overpressure is within 10 % difference of the maximum overpressure for short ignition delays.

The comparison of the different types of dispersion systems can also be done with dust particles of 40 μm in diameter. Figure 14 shows the results of maximum overpressure of the three different dispersion systems for a suspension of 40 μm dust. Once again a concentration of 600 g/m^3 of aluminum dust was used and the tests were performed for a wide range of ignition delays.

It can be seen that for the larger dust particles the behaviors of the different dispersion systems were quite distinct. The conical diffuser dispersion system yielded maximum overpressures significantly higher than the two other types of dispersion systems.

The conical diffuser dispersion system was designed to produce little turbulence in the combustion chamber. The dust sample was impacted by strong air jets in the external dust cup in order to break up the agglomeration of the dust grains, and the suspension then flowed slowly into the combustion chamber. The slow dispersion reduced swirling that could cause stratification of the suspension and impacting of the dust particles on the wall of the combustion chamber.

The other two types of dispersion systems relied on strong air jets to distribute the dust in the combustion chamber. When using these dispersion systems, the larger particles cannot follow the dispersion air stream lines and the suspension becomes depleted as the dust particles impact the wall of the combustion chamber.

Thus the level of turbulence intensity associated with the dispersion process is a determining factor in how the dust will follow the stream lines of the dispersion air. For slow air flows, the dust particles will follow the air more closely than for strong air jets.

It can also be observed from Figure 14 that the maximum overpressure decreases rapidly with the increase of the delay between dispersion and ignition. This indicates that settling is a strong factor when large dusts are dispersed. This high settling rate can be attributed to two main causes. First, the settling can be caused by the effect of gravity that pulls the dust particles to the bottom of the combustion chamber. The settling can also be the result of the removal of the dust due to the impacting of the dust particles on the wall of the combustion chamber.

3.1.2.3-The Determination of Intensity of Turbulence

The turbulence intensity of the dispersion process can be related to the burning rate of the produced suspension for short ignition delay. This means that for short ignition delays, the turbulence produced by the dispersion process increases the burning rate. This increased burning rate is manifested by an increase in the rate of pressure rise. From measurement of turbulent intensity, Pu [9,11] has shown a direct link between the rate of pressure rise and the turbulence intensity of the suspension. Turbulent eddies tend to promote mixing, thus increasing the burning rate [31]. As the burning rate increases, the rate of pressure rise increases accordingly.

Figure 15 shows the comparison of the rate of pressure rise for the three types of dispersion systems with respect to the ignition delay. The tests were done using 5.4 μm aluminum dust. It can be seen that for short ignition delay, the rate of pressure rise is greater for the Hartmann type dispersion system and the dispersion ring system than for the conical diffuser. This clearly indicates that the turbulence intensity of the dispersion process of the conical diffuser is lower than for the two other dispersion systems. These results confirm our initial expectation of the design of the conical diffuser dispersion system.

Comparing results with those from Figure 14, this substantiates that in order to create a more uniform suspension of large particles, a lesser turbulent dispersion system must be used.

3.1.3-Variation of the Size of the Dust Particles

The size of the dust particles used in performing the tests greatly influences the maximum overpressure as well as the maximum rate of pressure rise. The size of the dust particles acts in two distinct ways on the explosive characteristics of the suspension. First, there is a change in the way in which dust follows the flow of the dispersion air. As the dust particle size changes, this will have an effect on the drag to inertia ratio. The drag is proportional to the diameter of the dust particles, while the inertia is proportional to the mass or the volume of the dust particle. Thus, as the size of the particles increases, the inertia increases faster than the drag. The result being that as the size of the dust particles changes, their ability to follow the flow of the dispersion air jets will also change. This will influence the degree of stratification of the dust suspension and the amount of dust that will impact the wall of the combustion chamber. Therefore as the size of the dust particles increases, more dust will tend to impact the wall and come out of suspension, leaving less dust to participate in the combustion process. Less dust in the suspension translates to lower results of maximum overpressure.

The second way in which the size of the dust particles influences the maximum overpressure and the maximum rate of pressure rise is by changing the burning of the dust particles. Since burning of aluminum dust particles occurs on the surface of the particle, and because aluminum is non volatile, no gases are emitted as the particles are heated in the preheat zone of the flame. In this way burning takes place only at the surface of the dust particles [32,33]. As the flame reaches the surface of the particle, the intense heat can vaporize the aluminum and burning can occur in the gas phase, but the rate of heat transfer is still limited by the surface area of the dust particle.

The specific surface area of the dust grain is inversely proportional to the size of the dust particles. Therefore, by changing the dust particle size this will change the specific area on which burning can occur, influencing the rate of propagation of the flame front. For larger dust particles, the specific surface area being smaller than for smaller dust, the propagation of the flame front will be slower. The result being a lower rate of pressure rise.

The slower burning does not directly influence the quantity of dust that is burnt in such a way so as to not change the maximum overpressure. However, the longer propagation time permits for more settling of dust to occur thus reducing the maximum overpressure. This effect can be quite significant especially when the slow propagating speeds and the high settling rate of large dust are combined.

3.1.3.1-Results of Different Sizes Particles

Figure 16 shows the results of the maximum overpressure for different sizes of dust particles. The tests have been performed with different ignition delays in order to find the optimal dispersion conditions. The conical diffuser dispersion system is used because it has been proven to be the most adequate for burning a wide range of dust particle sizes.

It can be seen that the level of maximum overpressure decreases as the size of the particles increases. This indicates that less dust is burnt as the size of the dust increases. If all the types of dust were adequately dispersed, the level of overpressure would be the same. The fact that the level of overpressure is lower indicates that less dust is in suspension. The lower results of maximum overpressure of the large dust particles show that the difference in dispersibility of the various dusts is significant. Thus as the size of the dust particles increases, the efficiency of the dispersion system decreases and less dust is present in the suspension.

Figure 17 shows the different rates of pressure rise associated with the sizes of dust. The maximum rate of pressure rise is once again plotted against the delay between dispersion and ignition. The rate of pressure rise is much higher for the particles of 5.4 μm than for the particles of 18 or 40 μm. This is what was expected, since the specific surface area is smaller for the larger particles. The lower rates of pressure rise will also be due to the fact that less dust is present in the suspension when larger dust particles are used.

3.1.4-The Effect of Settling of the Dust Particles.

It was shown in the previous section that the combustion of large dust particles yielded low levels of maximum overpressure because large particles do not remain in suspension. It is of interest to attempt to establish the reasons for which the generation of a suspension of large particles is so troublesome.

3.1.4.1-Gravity Sedimentation of Dust

The inability of dust to stay in suspension can be attributed to two main causes. The most obvious cause is the effect of gravity. Dust particles in suspension are subject to the effect of gravity that tends to pull them towards the bottom of the combustion chamber. When the particles are out of the suspension, they no longer participate in the combustion process and the maximum overpressure is reduced.

The rate of settling due to gravity is counteracted by the drag that the air exerts on the particle. This means that as the size of the particles changes, it will influence the settling rate.

The concentration of particles also has an effect on the rate of settling. If the concentration of dust is high, the particles in the dust cloud do not fall as individual particles, but the interaction of the particles influences the rate of settling [34]. Experiments [35] show that settling rates may be twice the order of magnitude higher in suspension of high concentration than what was predicted for the falling of single particles. For example the settling velocity of particles of 5 μm is expected to be 5 cm/s (See Appendix C for discussion on Settling velocity). However, the settling velocity of a dense cloud of these same dusts can be as high as 1 m/s.

3.1.4.2-Removal of Dust Due to Turbulence

The other cause of the depletion of the suspension comes from the inability of the dust particles to follow the stream lines of the dispersion air jets. The dispersion systems used in this study rely on turbulent dispersion jets to distribute the dust particles inside the combustion chamber. These air jets tend to have a high curvature and in some cases dust particles cannot follow the stream lines of the dispersion flow. This results in a stratified suspension. The particles can become separated from the suspension if they impact and stick to the wall of the combustion chamber. The result of these two effects is a reduction in the maximum overpressure because less dust is burnt.

3.1.4.3-Determination of the Dominant Effect

In order to determine which effect is dominant, gravity settling or the separation of the dust due to swirling of the suspension, it is necessary to eliminate the driving force behind one of these settling mechanisms and observe the results. The sticking of dust caused by the swirling of the suspension is due to the inertia of the particles. Because inertia is an inherent property of mass, it is impossible to avoid such type of settling. If it were possible to reduce or eliminate the effect of gravity, then the settling due to gravity would no longer be an influencing factor. Thus in performing the experiments in a microgravity environment, the effect of gravity settling can be overlooked, in such a way that only reduction of dust concentration due to swirling of the suspension is present.

Figure 18 shows the results of maximum overpressure obtained in microgravity and in normal gravity. Both experiments were conducted using 5.4 μm dust in the sphere equipped with the conical diffuser dispersion system. The maximum overpressure is plotted against ignition delay to clearly show the effect of settling that occurs with time. It can be seen that in experiments performed in normal gravity, the maximum overpressure decreases as the delay between dispersion and ignition increases. This decrease in maximum overpressure indicates that less dust is being burnt meaning that less dust is in suspension. On the other hand, the results obtained in microgravity show no decrease in overpressure as the ignition delay is increased. This indicates that settling is not present in this second case. Because gravity settling cannot occur or is greatly reduced in microgravity, only sticking on the walls of the chamber due to swirling of the suspension can occur. Hence the microgravity results show that sticking of dust is not a significant factor when the 5.4 μm dust is used.

By comparing the two curves of Figure 18, it can be seen that the difference in maximum overpressure is due to the effect of gravitational settling alone. From these results it can be seen that the rate of settling due to gravity is quite significant since the deficit in maximum overpressure is appreciable for long delays.

Similar analysis can be done for particles of larger diameter. Figure 19 shows the maximum overpressure of aluminum of 40 μm in diameter in both normal and microgravity conditions. Once again the sphere used is equipped with the conical diffuser dispersion system. This dispersion system was used since it proved to be the most appropriate for burning the larger particles. The results of maximum overpressure are plotted against the ignition delay. Microgravity results show a decrease in maximum overpressure as ignition delay increases. The reduction in overpressure indicates that less dust is being burned. Because no gravitational settling of dust on the bottom of the combustion chamber can occur, the reduction of the concentration of dust must be due to the swirling of the suspension that causes the particles to impact and stick to the wall.

It can also be observed that the levels of maximum overpressure obtained in microgravity are significantly lower after one second delay than the level of maximum overpressure for shots of 50 ms ignition delay performed in normal gravity. The reason for this being that the initial suspension (right after the dispersion process has been completed) is highly turbulent and it is during this initial phase that most of the sticking of dust due to swirling is expected to take place. Thus for shots performed at extremely short ignition delays (50 ms), significant reduction in concentration from swirling of the suspension has not yet occurred, and more dust is burnt. Therefore the deficit in maximum overpressure of the microgravity results compared to the results obtained for short delays in normal gravity is due to intense swirling of the suspension.

The experiments performed in normal gravity show a fast decrease in maximum overpressure indicating that the settling rate is quite high. In ground based experiments, both gravity settling and sticking of dust particles on the wall of the combustion chamber due to swirling of the suspension occur. By comparing the results of maximum overpressure obtained on the ground and in microgravity, it can be seen that for short ignition delay times, the reduction of the quantity of dust due to swirling is significant. As for longer time delays, settling due to gravity becomes predominant. Thus for large dust particles both mechanisms of removal of dust from the suspension are significant.

3.1.5-The Effect of the Turbulent Scale of the Dispersion Jets

It has been shown that impacting of the dust particles with the wall of the combustion chamber tends to deplete the suspension. The dusts come out of suspension after the they have impacted the wall due to the inability of the dust particles to follow the curvature of the dispersion air. It has also been shown that different sizes of dust particles behave differently in air flows. Larger dusts do not follow the air flow as well as smaller dusts. Thus, suspensions of larger dust tend to become more depleted than suspensions of small dust.

The curvature of the dispersion air jets has a significant role in the rate of depletion of dust. The dust particles are able to follow flows of small curvature. In the limit of curvature that is zero, the dust will follow the straight air flow perfectly. However as curvature increases, the dust particles will be less able to follow the air flow. It is therefore of interest to study how the scale of the turbulent eddies of the dispersion process will influence this settling of the dust.

3.1.5.1-Determination of the Scale of Dispersion Jets

It is expected that if the vessel in which the dispersion is done has larger dimensions, the average scale of the turbulent dispersion eddies will also be larger. As seen before, the level of turbulence can be related to the burning rate, which is directly linked to the rate of pressure rise in a constant volume combustion chamber. So by comparing the different burning rates of the suspensions, it is possible to determine the relative turbulent intensity of the suspensions. Figure 20 shows the K_{St} for tests performed in a 4.4 liter sphere and a 35 liter combustion chamber. 40 μm aluminum dust was used in these tests, since it was proven to be the most sensitive to stratification of the suspension.

The K_{St} factor is related to the rate of pressure rise but normalized with the volume of the combustion chamber. The K_{St} is defined as:

$$K_{st} = \left(\frac{dP}{dt}\right)_{max} * V^{1/3} \tag{3.6}$$

where the rate of pressure rise is in bars per second and the volume in meters cubed. The K_{St} factor is closely related to the burning velocity. This is demonstrated in Appendix D. For this reason the K_{St} factor will be constant for the same combustible mixture that possess the same turbulence intensity. Because turbulence affects the burning velocity, it will also affect the K_{St}.

The K_{st} factor is plotted against ignition delay, to illustrate the variation of the rate of burning as time increases. It is observed that the K_{st} factor decreases faster in the 4.4 liter vessel than in the 35 liter vessel. The K_{st} factor is used instead of simply using the rate of pressure rise because there is a difference in the size of the combustion chamber.

From turbulent theory [36,37], it is known that the rate of dissipation of turbulence is inversely proportional to the scale of the turbulence. This means that small scale turbulence tends to decay faster than large scale turbulence. Since the K_{st} of the 4.4 liter combustion chamber decays faster, this indicates that the scale of the turbulence of the dispersion process is smaller in the 4.4 liter vessel than it is in the 35 liter vessel.

3.1.5.2-Results of Different Dispersion Scales

Having established the differences in the scale of the turbulence of the dust suspension, it is now possible to see the effect of the different flow fields on the maximum overpressure. Figure 21 shows the level of maximum overpressure for 40 μm aluminum dust for the two combustion chambers. The maximum overpressure is also plotted against the ignition delay. The maximum overpressure measured in the 35 liter vessel is significantly higher than in the 4.4 liter combustion chamber. This indicates that more dust is burnt in the 35 liter vessel, hence less settling has occurred. Because the scale of the turbulence is smaller in the 4.4 liter vessel, the dust cannot follow the flow and the dust impacts the wall of the combustion chamber. The resulting depleted suspension yields a lower maximum overpressure. The scale of the combustion vessel is thus a determining factor in maintaining the dust in suspension long enough for the combustion process to occur.

3.1.6-The Intensity of the Dispersion Process Compared to the Scale of the Dispersion Turbulent Jets

Because it has been determined that the intensity and the scale of the air of the dispersion air jets have an influence on the rate of depletion in the suspension, it must be found which of these two parameter has the greater effect. In order to compare these parameters, the results of maximum overpressure of the 35 liter vessel will be compared to the results obtained in the 5.4 liter sphere equipped with the conical diffuser dispersion system. The 35 liter vessel will be used because it has been shown to produce a suspension that is characterized by having a large scale of turbulence. The conical diffuser was used because this is the type of dispersion system that produced the least intense turbulent dispersion. Each of these systems offers an advantage in the creation of the suspension, and by comparing the results obtained, it will be possible to determine which of the two effects is the more important.

Figure 22 shows the results of maximum overpressure for the two types of combustion chambers using aluminum dust of 40 μm in diameter. The tests were performed over a wide range of ignition delays in order to be sure that the optimum value of delay is used to compare the results. Dust of 40 μm in diameter is used because it is the type of dust that is most sensitive to separation from the dispersion air flow.

It can be seen that the results in the smaller sphere are slightly higher than in the 35 liter sphere. This indicates that more dust is being burned in the small chamber than in the larger vessel. The fact that more dust remains in suspension in the smaller vessel shows that having a low level of turbulence intensity for the dispersion process is a more significant factor than a larger scale of the turbulence, in keeping dust suspended. Thus to produce suspensions of large dust particles, emphasis should be put on obtaining a suspension that will be created by jets that have a low dispersion intensity.

However, it is interesting to note that the optimal conditions in which a suspension can be created would be the combination of these two effects, that is to say, a dispersion system that has a low level of turbulence intensity combined with an average scale of turbulence that is large.

3.2-Visualization of the Dispersion Process

In order to portray the dispersion process of aluminum dust in a small scale spherical chamber, a photographic investigation has also been conducted. These experiments were performed in a transparent balloon to mimic the spherical combustion chamber. For the purpose of the dispersion process, the balloon was kept at constant volume and was rigid enough to contain the dispersion.

The experimental apparatus is quite similar to the apparatus that uses the conical diffuser with an external dust cup used for the combustion experiments. The angle and the dimensions of the diffuser cone are different in the two designs. This will create differences in the respective flow field of the dispersion air. As seen previously, different flow fields of the dispersion air creates different suspensions of dust.

Therefore, the aim of this section is to observe the general characteristics of a suspension during and after the dispersion process and not to attempt to reproduce any specific dispersion system.

3.2.1-Visualization of the Dispersion of 5.4 μm Dust

Figure 23 shows the transparent sphere just as the dispersion process is started. The smallest circle seen in the picture is the actual balloon, the larger circle seen is the window of the containment vessel. The dark rod in the bottom center of the sphere is the ignitor electrode. Note that the ignitor was not used in these experiments, only the dispersion process was observed. At the bottom of the sphere, on the left hand side of the ignitor electrode is the dispersion cone from which the dust suspension will flow. Dusts of 5.4 μm in diameter are used in this test and the air pressure used to disperse the dust is the same as in the combustion experiments. This is done in order to ensure that the suspension generated is similar to those of the combustion experiments.

Figure 24 shows the first stage of the dispersion as the dust is first injected into the combustion chamber. This image was taken 0.033 seconds after the dispersion was initiated. The dust cloud appears dense in the back lighting environment because it is still at a high concentration, as significant mixing has not yet occurred. Note that at this point, the dust suspension has not yet interacted with the wall of the transparent chamber.

As time progresses, mixing occurs in the sphere. At 0.066 and 0.099 seconds (Figures 25 and 26) the suspension seems completely uniform. If gravity settling was significant, it would be expected that the concentration would be higher at the bottom of the sphere, but in actuality it can be seen that little dust is found at the bottom section of the chamber. This is due to the fact that the dispersion process is in the upward direction and only by mixing will the dust eventually be distributed in the lower section of the chamber.

Figure 27 shows that after 0.026 seconds the suspension seems to be completely uniform. Turbulent mixing has evenly distributed the dust in the sphere and no more clear areas appear. It must be noted that since back lighting was used, the information recorded is integrated over the whole depth of the sphere. This means that many inhomogeneities can still occur in the suspension even though the suspension looks uniform from the side. Therefore the results of uniform suspension must be seen in a global view, keeping in mind that localized zones of non uniform concentrations can occur.

This exercise shows, as expected from the results of combustion, that a relatively uniform suspension of 5.4 μm dust is easily obtained in the chamber. This illustrates clearly the reasons for the high results of maximum overpressure that were consistently obtained with the small dust particles. This dust was easily dispersed and the resultant suspension always contained a large quantity of dust.

3.2.2-Visualization of the Dispersion of 40 μm Dust

The same procedure was performed for dust of 40 μm in diameter. This is done to observe the variation in the time evolution of the suspension for different dusts. Figure 28 shows the sphere at the onset of dispersion. After 0.033 seconds into the dispersion, the dust had started to flow into the sphere (Figure 29). Figure 30 shows the dispersion after 0.066 seconds. As seen in Figure 30, the 40 μm dust barely occupies half of the sphere. It is interesting to notice that at this point in time, the suspension of 5.4 μm dust occupied most of the sphere.

Figure 31 illustrates the dust cloud hitting the wall of the sphere on the right hand side of the picture. The suspension has grown only marginally in the rest of the sphere since the previous frame. After 0.267 seconds the suspension of 5.4 μm dust was uniform. Figure 32 shows the suspension of 40 μm dust particles for the same time. It can be seen that hardly any significant amount of dust is found in the suspension.

Figures 33 and 34 show the suspension at 0.33 and 0.5 seconds respectively. No notable amount of dust is found in the spherical chamber, which explains the extremely low results of maximum overpressure that were obtained in the tests when the 40 μm aluminum dust was used in the combustion vessels.

By examining Figures 28 to 34 in sequence, it can be seen that no suspension is actually created. The dust is never suspended in air. It is injected in the vessel and it settles almost instantly. This further explains the scattering of the results of maximum overpressure obtained when the 40 μm dust is used. From one shot to another, the amount of dust the ignitor is exposed to can be quite dissimilar, yielding different levels of maximum overpressure.

4-Summary and Conclusions

4.1-Summary of Results

A systematic investigation of the effect of the size of the dust particles on dust explosions has been conducted. The experiments performed were done under many different experimental conditions in order to establish the effect of all the parameters that were involved. The following is a summary of the results found.

The effect of the type of dispersion system was looked at. This illustrated the effect that had different flow fields of dispersion air on the maximum overpressure. Results for different dispersion systems with 5.4 μm dust show that the maximum overpressure were equivalent for all the dispersion systems. This indicates that small dusts are able to follow the dispersion flow well enough to be dispersed by any type of dispersion system. When 40 μm dust was tested, the results showed that the conical diffuser yielded significantly higher results of maximum overpressure. The reason for this proved to be the fact that the suspension created by the conical diffuser is less turbulent and that less dust came out of suspension due to swirling of the suspension.

The effect of dust particles size was then studied. It was shown that the maximum overpressure decreased significantly with the increase of the size of the dust particles. This was attributed to a reduction in the efficiency of the dispersion system with increasing dust particle size. Less dust in the suspension yields lower results of maximum overpressure. Results also showed that the rate of pressure rise was significantly reduced. This second effect was caused by the reduction of specific surface are associated with larger dust. The fact that there was less dusts present in the suspension also reduced the rate of pressure rise.

The effect of settling of dust particles was studied. In order to establish if the decrease in dust concentration due to the impacting and the sticking of the dust particles was significant compared to gravity settling, tests in microgravity were performed. The results showed that sticking due to swirling of 5.4 μm dust particles was negligible. The gravity settling had an effect, but only after many seconds of ignition delay (typically ≈10 seconds). For large dust, both effects were significant. The removal of dust was done in two periods. The initial period where the suspension was quite turbulent was characterized by high rates of removal of dust due to separation and sticking of the dust. After the initial stage of dispersion, gravity settling was the dominating factor. Microgravity results also showed that sticking of dust due to swirling still occurred during many seconds after the dispersion was done.

The influence of the scale of the dispersion eddies was also investigated. It was shown that large dust was unable to follow dispersion eddies that had a small scale and that the maximum overpressure was lower because less dust was present in suspension. Next, the effect of the scale of the dispersion jets was compared to the effect of the intensity of the dispersion process. This showed that having a dispersion process of lower dispersion intensity had a bigger influence than the scale of the dispersion eddies.

Finally, a photographic investigation of the dispersion process was performed. This permitted the observation of the development of a dust suspension as it was generated by the dispersion system. It was found that the generation of a suspension of particles of 5.4 μm dust was quite efficient. However, when an attempt was made to generate a suspension of dust particles of 40 μm, it was observed that a suspension was never obtained and that the dust tended to settle almost instantly.

4.2-Concluding Remarks

The influence of the size of the dust particles on dust explosion was mainly felt in the difference in the dispersibility of the dust. The reduction in maximum overpressure was due to the reduction in concentration of dust caused by the decrease in the efficiency of the dispersion system. The decrease in the specific surface area combined with the reduction of the amount of dust present in the suspension accounted for the decrease in rate of pressure rise.

The reduction in dispersion efficiency was caused by the inability of the dust particles to follow the stream lines of the dispersion air jets. Depending on the intensity of the dispersion jets and the scale of the dispersion system used, the results of maximum overpressure varied. For large dust particles (40 μm), it was found that the ideal type of dispersion system would combine a low level of turbulent intensity while having turbulent eddies of large scale. Emphasis must be put on a system that possesses a low level of turbulent intensity since this was found to have a stronger effect on the rate of removal of dust due to impacting with the wall of the chamber. However, when small (5.4 μm) particles were used, the influence of the conditions in which experiments were performed was quite small.

The conclusion from these findings, is that the explosion potential of larger dusts tends to be under estimated. In performing tests to determine the explosive potential of a dust suspension, the dispersion system is assumed to adequately perform its task. This is usually true for particles of small diameters. Problems arise when larger dusts are used. The efficiency of the dispersion system becomes much lower than what it was for smaller particles. Because there is less dust in suspension the results of maximum overpressure and maximum rate of pressure rise will be low and thus the suspension will be classified incorrectly as having a low explosive potential. For this reason great care must be use when testing larger dust particles especially in terms of ascertaining the quality of the suspension.

References

1) Bartknecht, W., **"Explosions-Course-Prevention-Protection"** Translated by H.Burg and T. Almond, Springer- Verlag Publishing Co., New York, 1989.

2) Hertzberg, M. and Cashdollar , K. L., **"Introduction to Dust Explosions"** *Industrial Dust Explosions*, ASTM STP 958, Kenneth L. Cashdollar and Martin Hertzberg, Eds., American Society for Testing and Materials, Philadelphia, 1987, pp 5-32.

3) Lee, J. H. S., **"Dust Explosion Parameters, their Measurement and Use"**, *Kolloquium Sichere Handhabung Brennbarer Stäube*, Verein Deutscher Ingenieure VDI, Nüremberg, 1988.

4) Lee, J. H. S., **"Dust Explosions: An Overview"**, *Shock Tubes an Waves, Proceedings of the Sixteenth International Symposium on Shock Tubes and Waves*, Achen, West Germany, 1987.

5) Nagy, J. and Verakis, H. C., **"Development and Control of Dust Explosions"**, Marcel Dekker, inc., New-York and Basel, 1983.

6) Makris, A., **"Lean Flammability Limits of Dust-Air Mixtures"**, Master Thesis, McGill University, Montreal, Canada, 1988.

7) Bartknecht, W., **"Preventive and Design Measures for Protection Against Dust Explosions,"** *Industrial Dust Explosions*, ASTM STP 958, Kenneth L. Cashdollar and Martin Hertzberg, Eds., American Society for Testing and Materials, Philadelphia, 1987, pp 158-190.

8) Conti, R. S. and Hertzberg, M., **"Thermal Autoignition Temperatures from the 1.2-L Furnace and Their Use in Evaluating the Explosion |Potential of Dusts"** *Industrial Dust Explosions*, ASTM STP 958, Kenneth L. Cashdollar and Martin Hertzberg, Eds., American Society for Testing and Materials, Philadelphia, 1987, pp 45-59.

9) Pu Y. K. et al., **"The Investigation of the Feature of Dispersion Induced Turbulence and its Effects on Dust Explosions in Closed Vessels"**, *Twenty*

Second Symposium (International) on Combustion, The Combustion Institute, 1988, pp 1777-1787.

10) Bond J. K. et al., **"Influence of Turbulence on Dust and Gas Explosions in Closed Vessels"**, *Tenth ICDERS Proceedings,* Berkley, California, American Institute of Aeronautics and Astronautics, 1986.

11) Pu Y. K. et al., **"Determination of Turbulent Parameters in Closed Explosion Vessels"**, *Twelfth ICDERS Proceedings,* Ann harbor, Michigan, American Institute of Aeronautics and Astronautics, 1990.

12) Lee, J. H. S., **"Influence of Turbulence on Closed Volume Explosion of Dust-Air Mixture"**, *Archivum Combustionis,* Vol 7, No. 3/4, 1987.

13) Rzal, F. et al., **"Experiments on Turbulent Flame Propagation In Dust-Air Mixtures"**, *Thirteenth ICDERS Proceedings,* Nagoya, Japan, American Institute of Aeronautics and Astronautics, 1992.

14) Itoh, S. et al., **"Basic Research on Combustion Characteristics of Micronized Coal"**, *ASME/JSME Thermal Engineering Proceedings,* Volume 5, 1991, pp 79-86.

15) Van der Wel, P. et al., **"A Study of Particle Factors Affecting Dust Explosions"**, *Particles and Particulate System Characteristics,* Vol 8, 1991, pp 90-94.

16) Fan, B.C. et al., **" An Aluminum Dust Explosion in a Spherical Closed Vessel"**, *Proceedings of the Fifth International Colloquium on Dust Explosions (Supplement),* Piotr Wolanski Ed., Warsaw. 1993, pp 21-29.

17) Shames, I. H., **"Mechanics of Fluids"**, McGraw Hill Book Co., New York, 1982.

18) Lee. J. H. S. et al, **"Microgravity Combustion of Dust in a Spherical Chamber"**, *Eighth European Symposium on Materials and Fluid Science in Microgravity,* Brussels, Belgium, 1992.

19) Ballal, D. R., **"Flame Propagation Through Dust Clouds of Carbon, Coal, Aluminum and Magnesium in an Environment of Zero Gravity"**, *Proc. R. Soc. Lond,* A 385, pp 21-51, 1983

20) Ross, H. D. et al., **"Feasibility of Reduced Gravity Experiments Involving Quiescent Uniform Particle Cloud Combustion"**, *NASA Technical Memorandum,* 101371, 1989.

21) Gieras, M. and Wolanski, P., **"Flame Propagation and Extinction in Hybrid Mixtures at Micro Gravity and Normal Gravity Conditions"**, *Archivum Combustionis,* Vol. 12, No. 1-4, 1992.

22)Ronney, P. D. and Wachman, H. Y., **"Effect of Gravity on Laminar Premixed Gas Combustion I: Flammability Limits and Burning Velocities"**, *Combustion and Flame,* Vol. 62, pp 107-119, 1985.

23)Ronney, P. D., **"Effect of Gravity on Laminar Premixed Gas Combustion II: Ignition and Extinction Phenomena"**, *Combustion and Flame,* Vol. 62, pp 121-133, 1985.

24)Williams, B. and White, L., **"NASA JSC Reduced Gravity Program User's Guide"**, *NASA Publications,* September, 1990.

25) Hartmann, I. et al., **"Inflammability and Explosibility of Metal Powders"**, *U.S. Bureau of Mines, Report of Investigation,* RI 3772, 1943.

26)Lee, J.H.S and Peraldi, O., **"Microgravity Combustion of Clouds, Phase III"**, Final Progress Report, CSA Contract # 9F007-2-6026/01-SW, 1993.

27) Fuks, N. A., **"The mechanics of aerosols"**, translated from the Russian by R. E. Daisley and Marina Fuchs ; translation edited by C. N. Davies, New York, Macmillan, 1964.

28) Jacobson, M. et al., **"Explosibility of Metal Powders"**, *U.S. Bureau of Mines, Report of Investigation,* RI 6516, 1964.

29) Ishihama, W. and Enomoy, H. **"Experimental Study of the Explosion Characteristics of Metal Dust Clouds"**, *Fifteenth Symposium (International) on Combustion* , Tokyo, Japan, 1974, pp 479-487.

30) Perlee, H. E. et al., **"Constant Volume Flame Propagation"**, *U.S. Bureau of Mines, Report of Investigation*, RI 7839, 1974.

31) Johnson, J. A. et al. **"Turbulence in a Reacting Contact Surface"**, *Physics of Fluids A*, Volume 2, Number 11, November 1990.

32) Cassel, H. M., **"Some Fundamental Aspects of Dust Flames"**, *U.S. Bureau of Mines, Report of Investigation*, RI 6551, 1964.

33) Steinberg, T. A. et al., **"The Combustion Phase of Burning Metals"**, *Combustion and Flame*, Volume 91, 1992, pp 200-208.

34) Boothroyd, R. G., **"Flowing Gas-Solids Suspensions"**, Chapman and Hall ltd., London, 1971.

35) Greene, F. T. and O'Donnel, J. F., **"The Quenching Behavior of Coal Dust-Air Mixtures"**, Bureau of Mines, OFR 4-83, August, 1981.

36) Lesieur, M., **"Turbulence in fluids: stochastic and numerical modeling"**, Dordrecht; Boston: Kluwer Academic Publishers, 1990.

37) Batchelor, G. K., **"An Introduction to Fluid Dynamics"**, Cambridge University Press, London, 1967.

38)[1] Bradley, D. and Mitcheson, A., **"Mathematical Solutions for Explosions in Spherical Vessels"**, *Combustion and Flame*, Volume 26, pp 201-217, 1976.

---

[1]Found in Appendix C

Appendix A

In order to have a pressure of one atmosphere in the combustion chamber after the dispersion process has occurred, it is necessary that the pressure in the combustion chamber be sub-atmospheric prior to the dispersion process because air jets are used to disperse the dust. The following describes the method used to calculate the initial pressure inside the combustion chamber with respect to the dispersion pressure used to disperse the dust. The 4.4 liter dispersion ring chamber will be considered in this case, but the same procedure applies for all the other systems.

The volume of the combustion chamber is 4.4 liter. The volume of the high pressure dispersion chamber is 0.2 liter. Defining:

$$V_{cc}=4.4 \text{ liter} \tag{A.1}$$

$$V_{hp}=0.2 \text{ liter} \tag{A.2}$$

The dispersion pressure used for all the experiments was 4.8 bars. Knowing this, the initial pressure in the combustion chamber must be calculated.

$$P_{cc} * V_{cc} + P_{hp} * V_{hp} = P_{total} * V_{total} \tag{A.3}$$

$$P_{total} = 1 \text{bars} \tag{A.4}$$

and

$$V_{total} = V_{cc} + V_{hp} \tag{A.5}$$

$$P_{cc} * V_{cc} + P_{hp} * V_{hp} = 1 \text{bars} * \left(V_{cc} + V_{hp}\right) \tag{A.6}$$

Knowing $V_{cc}, V_{hp} \& P_{hp}$

$$P_{cc} * 4.41 + 4.8bars * 0.21 = 1bars * (4.41 + 0.21) \quad \text{(A.7)}$$

$$P_{cc} = \frac{1bars * (4.41 + 0.21) - 4.8bars * 0.21}{4.41} \quad \text{(A.8)}$$

$$P_{cc} = 0.83bars \quad \text{(A.9)}$$

So in order to obtain atmospheric condition in the combustion chamber prior to ignition, the pressure before the dispersion process is performed must be 0.82 bars, for a dispersion pressure of 4.8 bars.

Appendix B

The stoichoimetric reaction of aluminum in air is found by balancing the amount of aluminum and air required to form the product of reaction alumina. There is also presence of nitrogen in the products, because in a calculation of the stoichoimetric conditions, it is assumed that the nitrogen does not participate in the reaction. The stoichoimetric reaction is shown below:

$$2\mathrm{Al} + \frac{3}{2}\left(\mathrm{O_2} + 3.76\mathrm{N_2}\right) \rightarrow \mathrm{Al_2O_3} + 5.64\mathrm{N_2} \tag{B.1}$$

where

$$\frac{3}{2}\left(\mathrm{O_2} + 3.76\mathrm{N_2}\right) = \frac{3}{2} \times 4.76 \text{ moles of air} = 7.14 \text{ moles} \tag{B.2}$$

thus

Two moles of Al for 7.14 moles of air

The molecular weight of aluminum is 26.98 g/mole. The volume of 7.14 molecules of air can be found by using the perfect gas law as:

$$PV = n \cdot \Re \cdot T \tag{B.3}$$

thus

$$V = \frac{n \cdot \Re \cdot T}{P} \tag{B.4}$$

where:

$$n = 7.14 \text{ moles} \tag{B.5}$$

$$T = 298 \text{ K} \tag{B.6}$$

$$\Re = 8.314 \ \frac{\mathrm{J}}{\mathrm{K} \cdot \text{mole}} \tag{B.7}$$

and

Appendix C

By performing a force balance on a small sphere falling in a viscous liquid equation C.1 arises. The first term of the equation represents the weight of the object or the force that gravity exerts on its mass. The second term of the expression is the buoyancy force that the fluid in which the sphere is falling exerts on the sphere. This term is usually negligible since the density of the sphere is usually much greater than the density of the sphere when metal spheres are falling in air. Nevertheless, this term will be conserved for the calculations. The last term of the equation is the viscous drag force that is applied to the sphere. This is the expression of Stoke's drag [17]. This applies for low Reynold's number, i.e. high viscosity, low velocity and objects of small dimensions. The case of dust settling in air is a good example. It must be noted that the equilibrium of these terms represents the terminal or settling velocity of the sphere and is denoted by the equality to zero.

$$\frac{4}{3}\cdot\pi\cdot R^3\cdot\rho_s\cdot g-\frac{4}{3}\cdot\pi\cdot R^3\cdot\rho_L\cdot g-6\cdot\pi\cdot\mu\cdot V_T\cdot R=0 \tag{C.1}$$

By modifying this equation it is possible to obtain the explicit expression for the terminal velocity as:

$$V_T=\frac{\frac{4}{3}\cdot R^2\cdot\rho_s\cdot g-\frac{4}{3}\cdot R^2\cdot\rho_L\cdot g}{6\cdot\mu} \tag{C.2}$$

Plotting the terminal velocity or the velocity at which the dust particles will fall, the following graph is obtained:

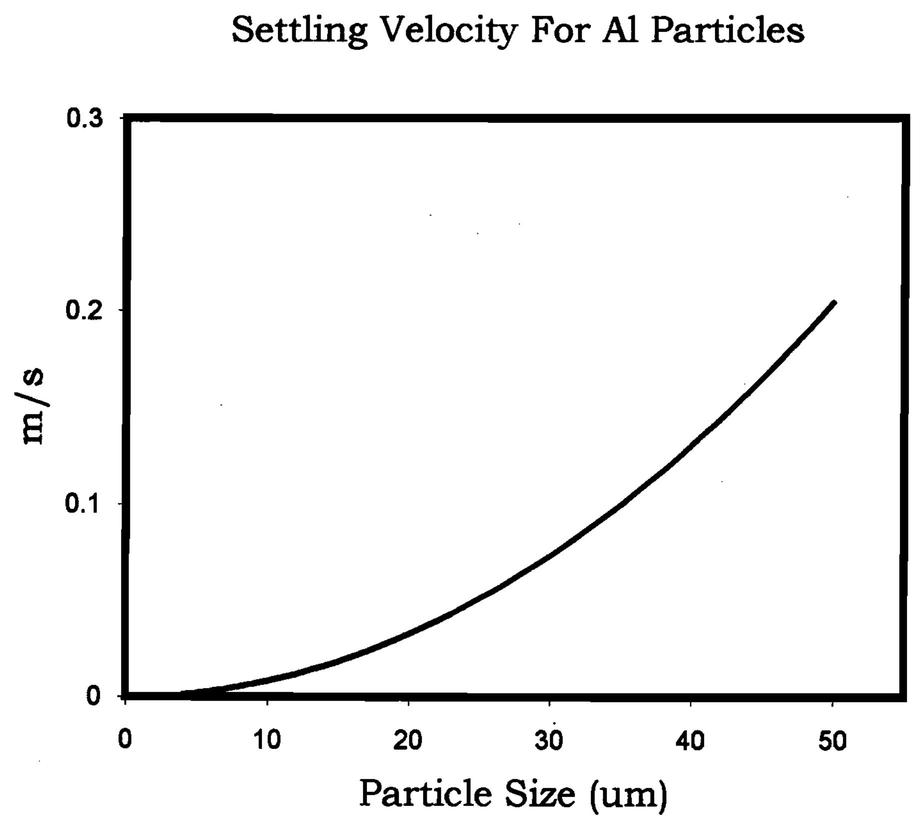

Figure C.1

The quadratic character of the curve can be clearly observed. This demonstrates well that has the size of the dust particles increases the settling velocity of the dust particles increases even faster. The result of which is that large dust particles have quite high settling velocities compared to small particles.

Appendix D

Bradley and Mitcheson [38] found that the burning velocity of a gas mixture in a constant volume process could be found from the pressure in the chamber and the rate of pressure rise. The form of the relation found is:

$$S = \frac{R}{3} * \left(\frac{dP}{dt}\right)_{max} * \frac{1}{\Delta P_{max}} * \left(\frac{\Delta P}{P_o} + 1\right)^{-1/\gamma} * \left\{1 - \left(1 - \frac{\Delta P}{\Delta P_{max}}\right) * \left(\frac{P_o}{\Delta P + P_o}\right)^{1/\gamma}\right\}^{-2/3} \quad \text{(D.1)}$$

By comparing the expression of burning velocity derived by Bradley and Mitcheson and the expression for the K_{st}:

$$K_{st} = \left(dP/dt\right)_{max} * V^{1/3} \quad \text{(D.2)}$$

it is clear that there exists a very close relationship between the two values. Both the K_{st} and the burning velocity (S) are proportional to the maximum rate of pressure change and they both depend on the cubic root of the volume of the combustion chamber, which is equivalent to the radius of the combustion chamber. The burning velocity has some additional parameters that are constant when the maximum case is considered. The burning velocity of a mixture remains constant independent of the volume of the combustion chamber, so it is expected that the K_{st} factor be constant for a given mixture. In order to compare the rate of propagation of the flame front in chambers of different sizes, it is important to compare the K_{st} rather than simply the $(dP/dt)_{max}$, because the K_{st} is normalized with the volume of the combustion chamber.

Figures

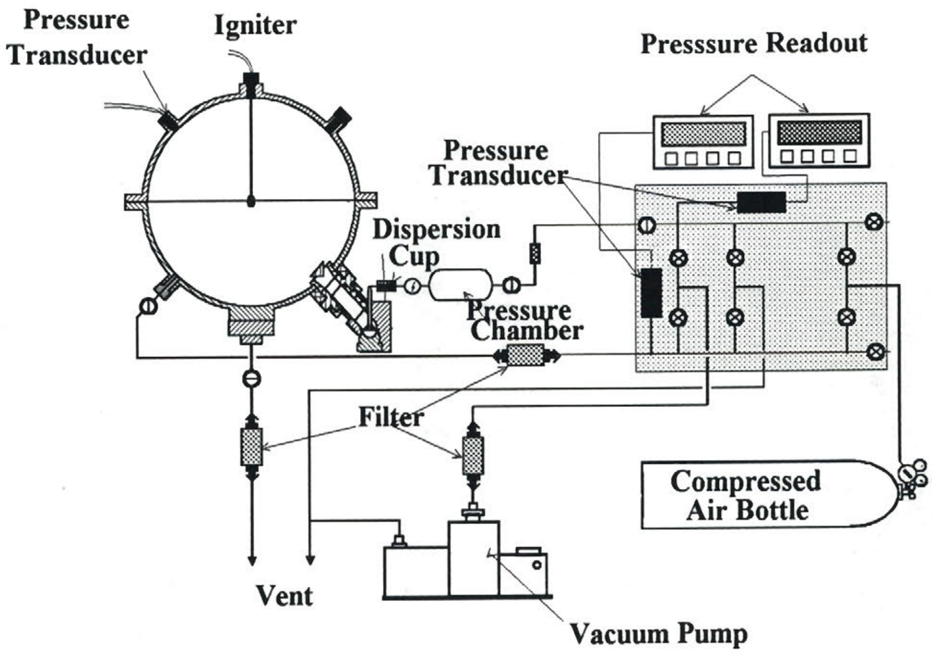

Figure 1: Typical layout of experimental setup with combustion chamber and control panel

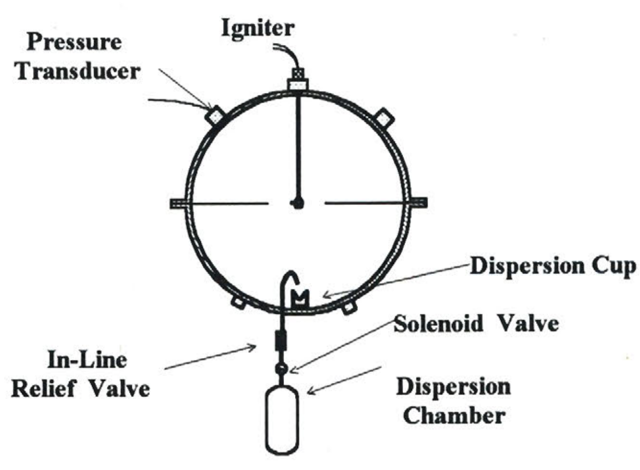

Figure 2: 4.4 liter Hartmann type combustion chamber

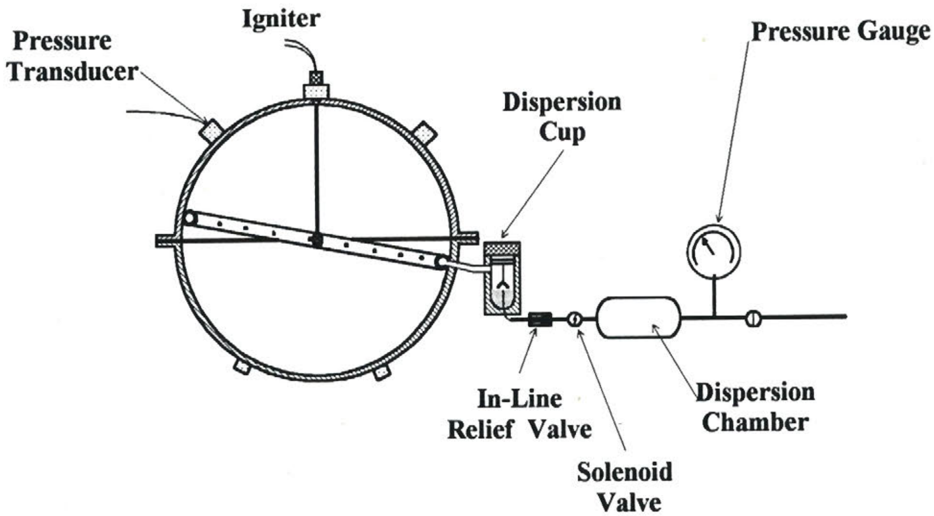

Figure 3: 4.4 liter combustion chamber with dispersion ring.

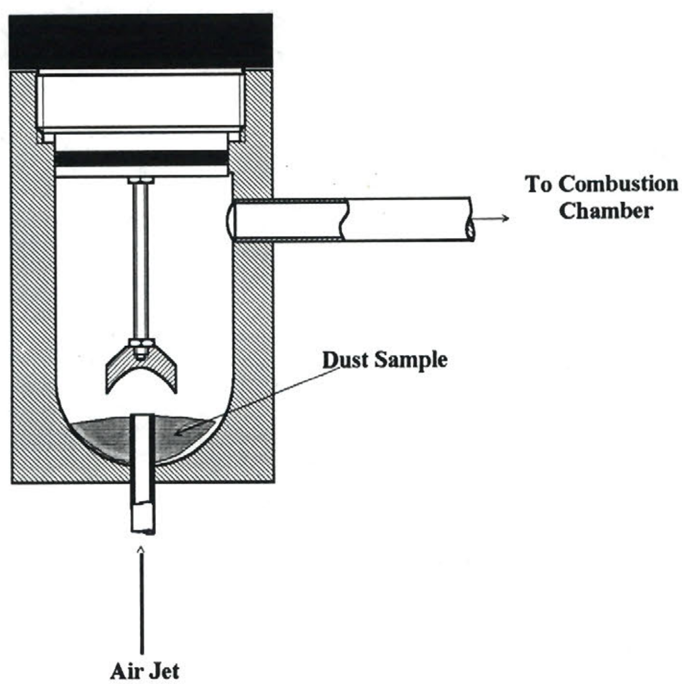

Figure 4: Detailed view of the dispersion cup used to generate the suspension of dust to be dispersed by the dispersion ring.

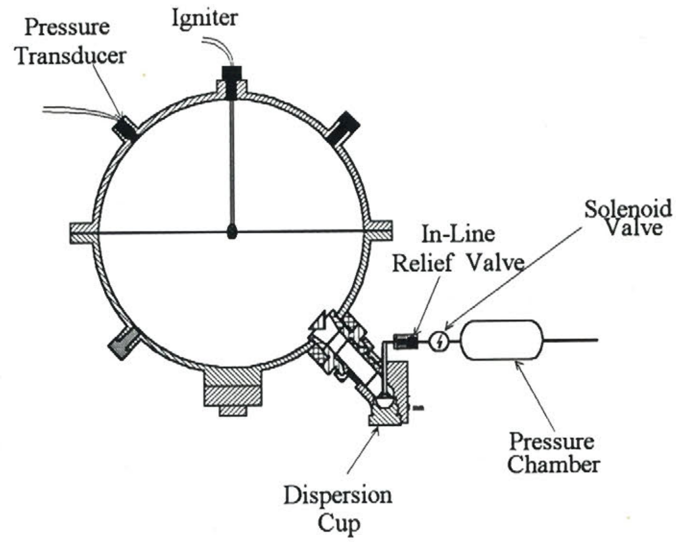

Figure 5: 5.4 liter combustion chamber equipped with a conical diffuser and external dust cup.

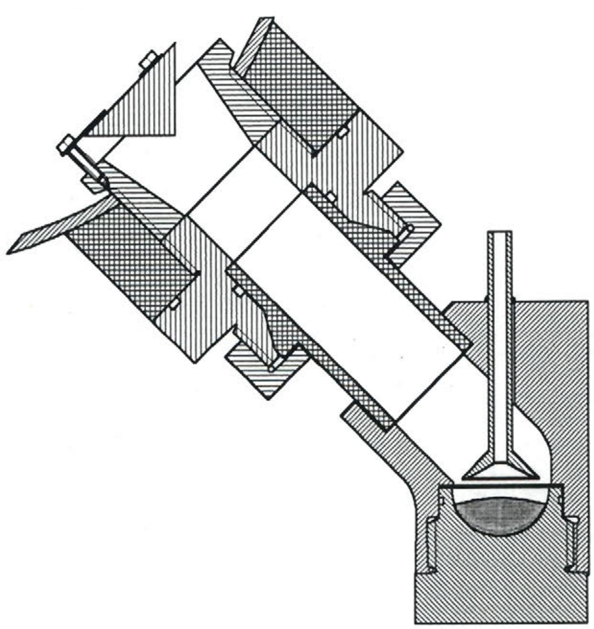

Figure 6: Detailed view of the dust cup and the conical diffuser used in with the 5.4 liter combustion chamber.

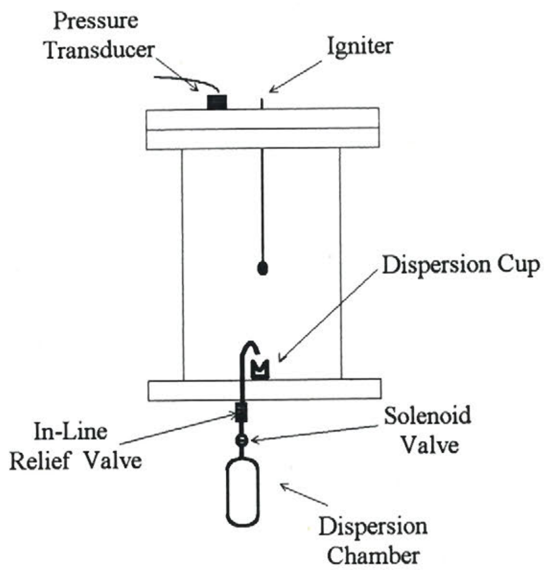

Figure 7: 35 liter combustion chamber assembly with Hartmann type dispersion system.

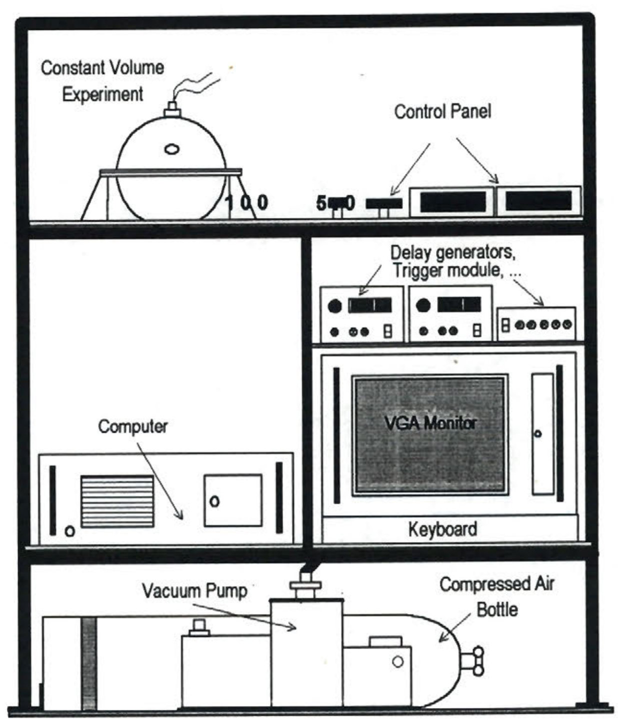

Figure 8: Schematic of the microgravity laboratory rack assembly.

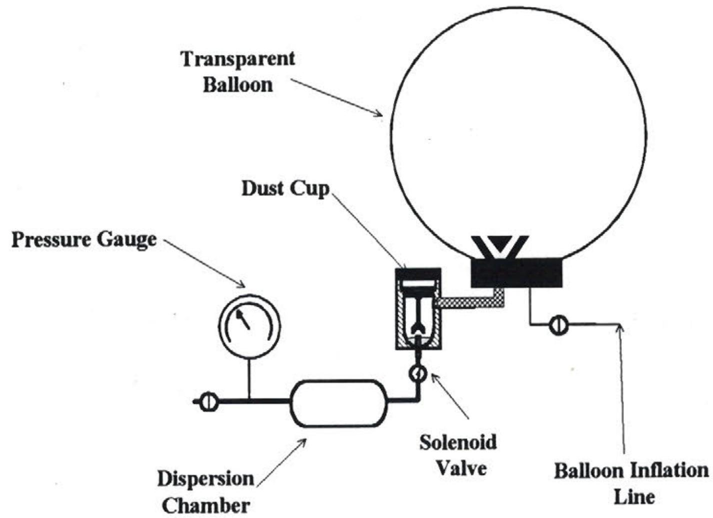

Figure 9: Dispersion visualization chamber assembly.

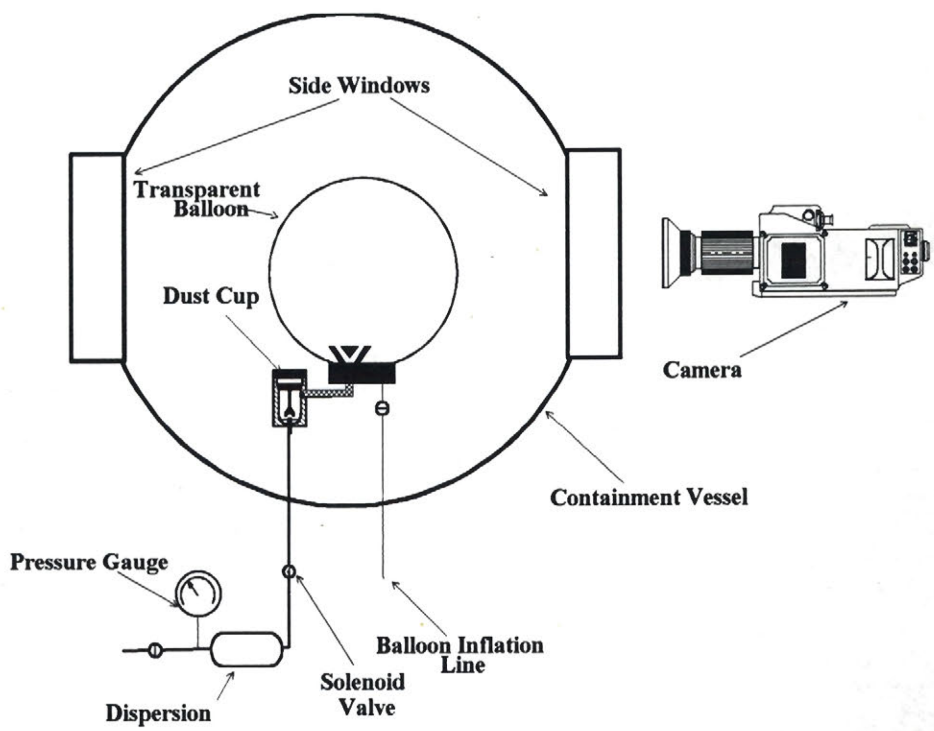

Figure 10: Dispersion visualization chamber and containment vessel assembly.

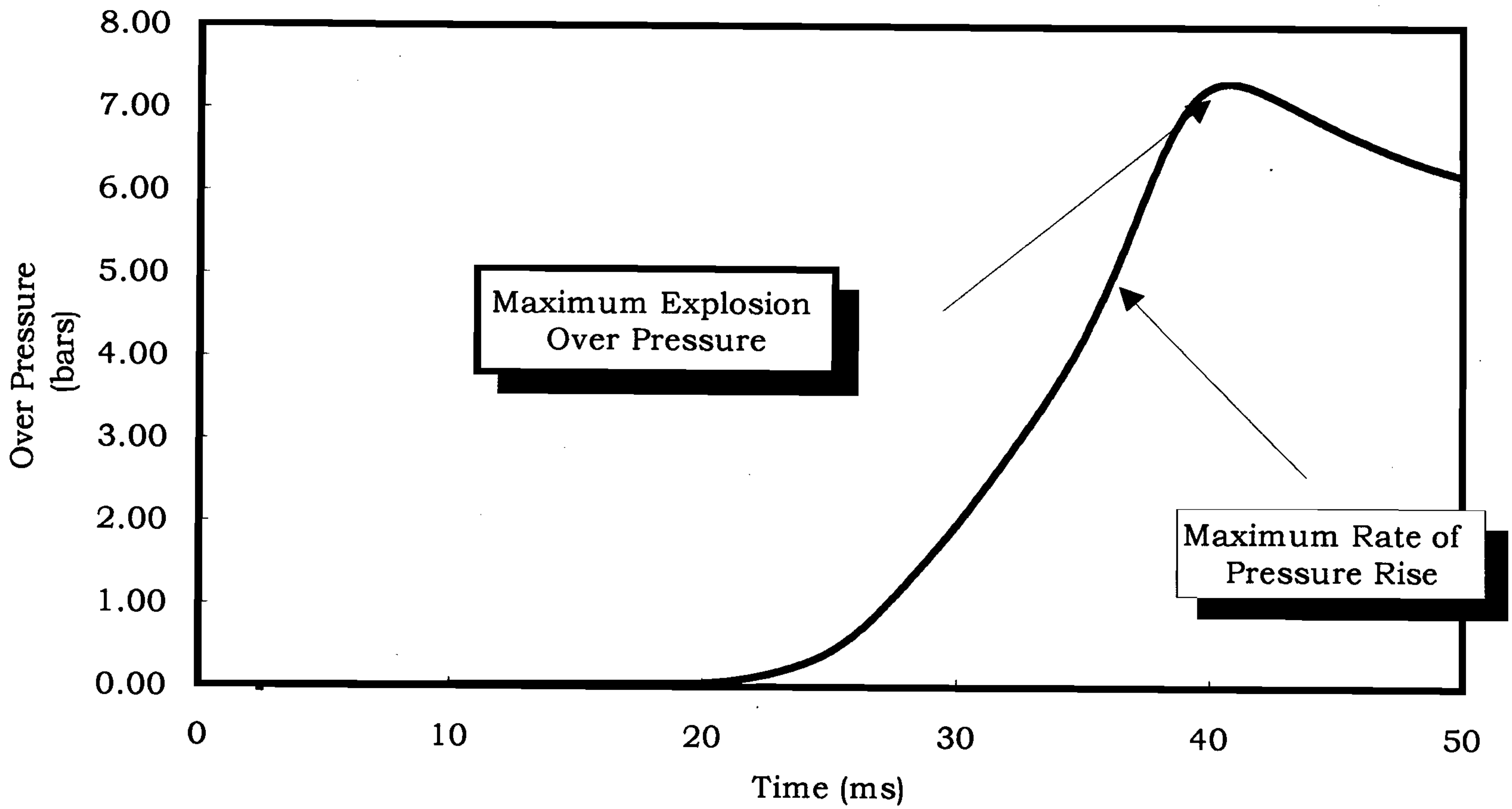

Figure 11: Sample pressure trace obtained for 5.4 μm aluminum dust using the Hartmann type dispersion system in the 4.4 liter sphere.

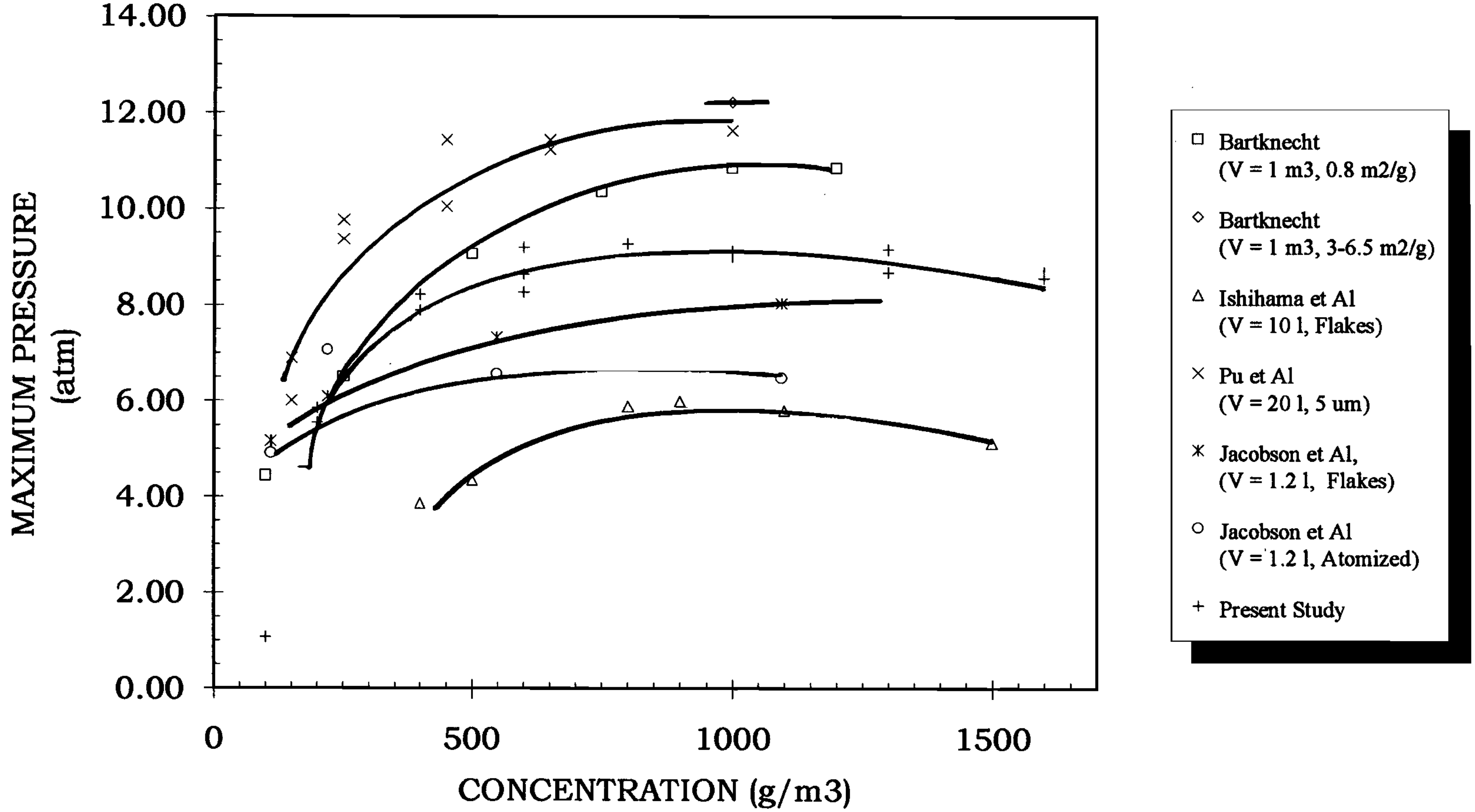

Figure 12: Maximum constant volume explosion pressure of aluminum-air suspensions for different experimental configuration.

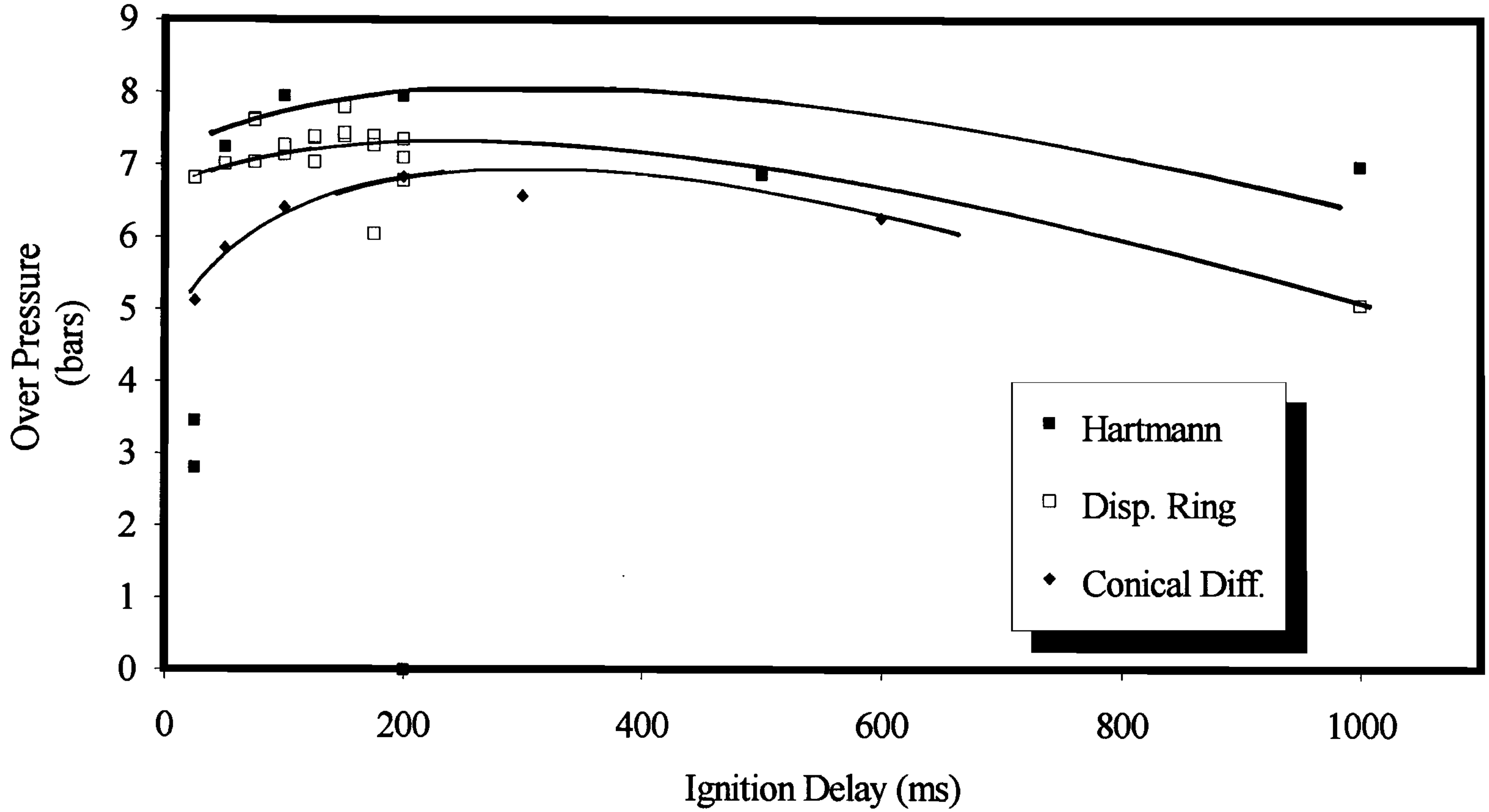

Figure 13: Results of maximum overpressure for different types of dispersion systems using aluminum dust of 5.4 μm.

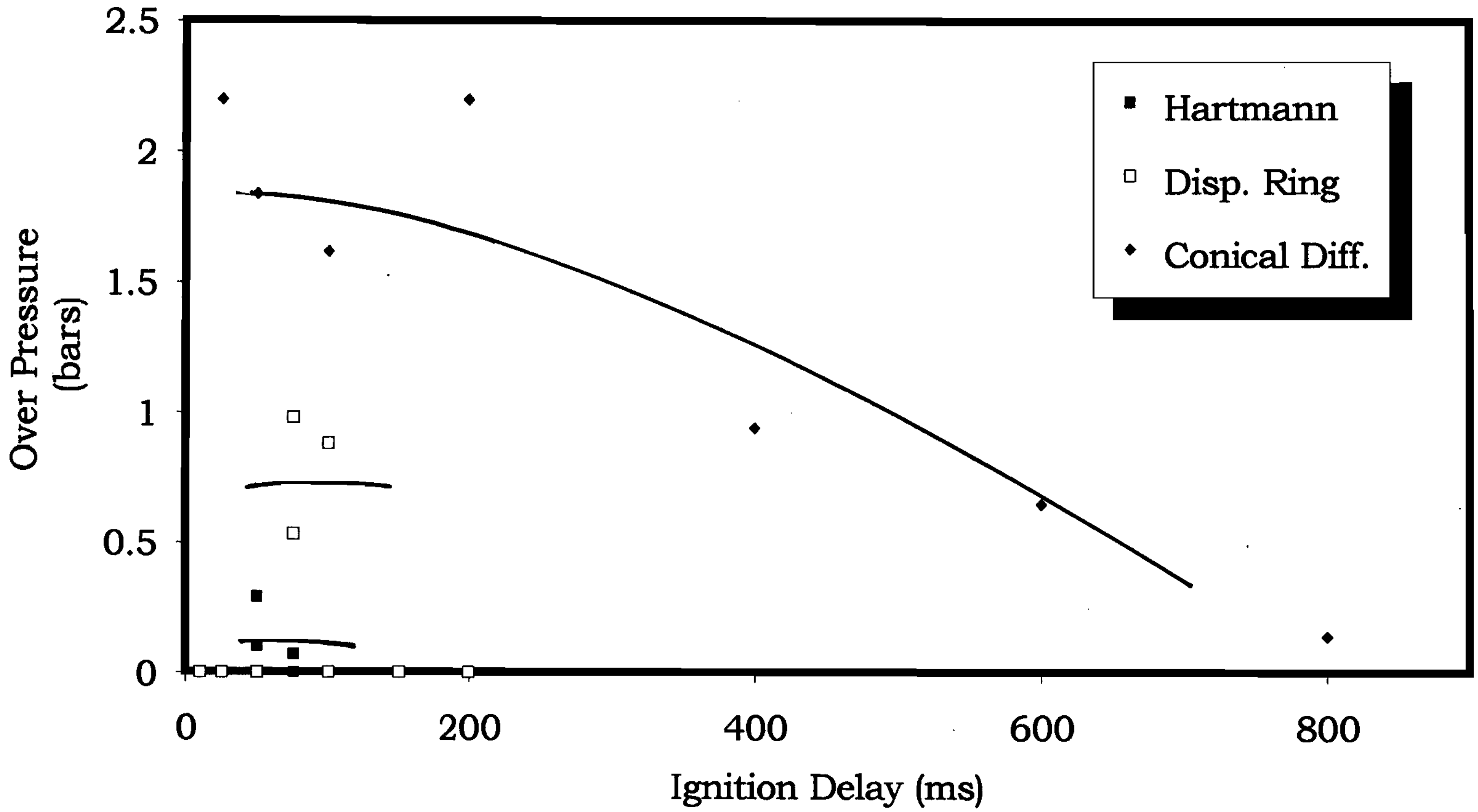

Figure 14: Results of maximum overpressure for different types of dispersion systems using aluminum dust of 40 μm.

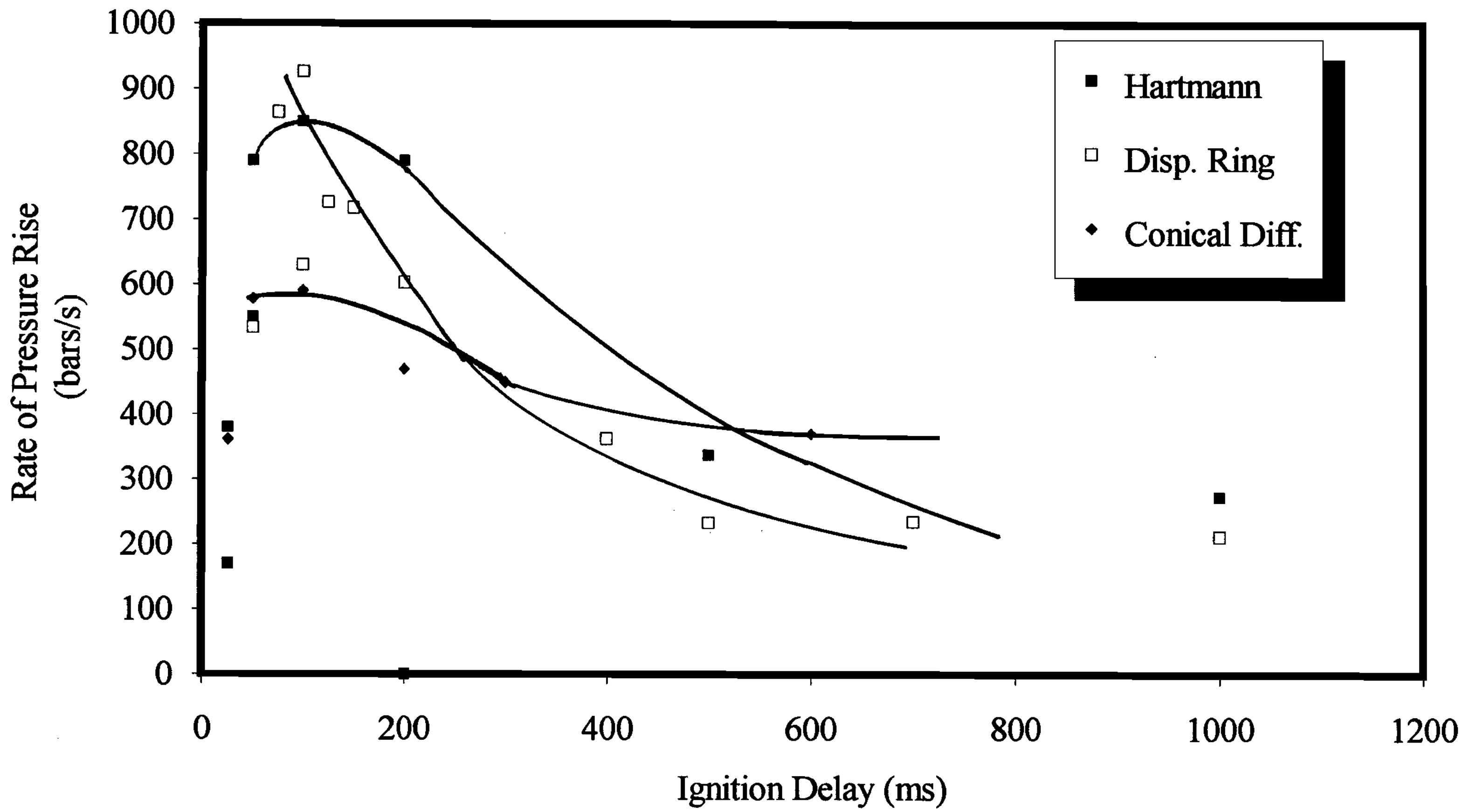

Figure 15: Results of maximum rate of pressure rise for different types of dispersion systems using Aluminum dust of 5.4 μm diameter.

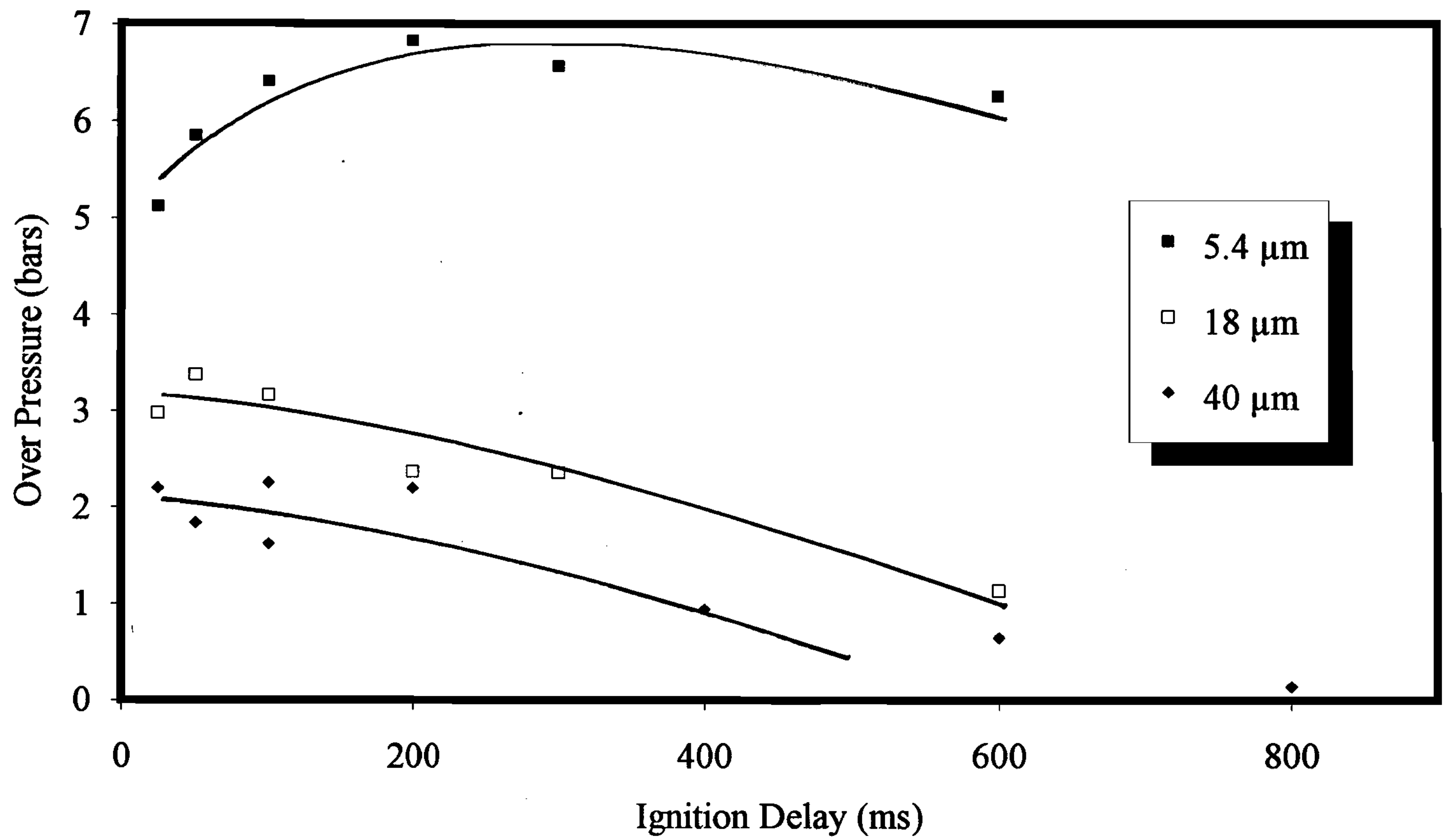

Figure 16: Results of maximum overpressure using different sizes of Aluminum dust particles, dispersed using the conical diffuser dispersion system.

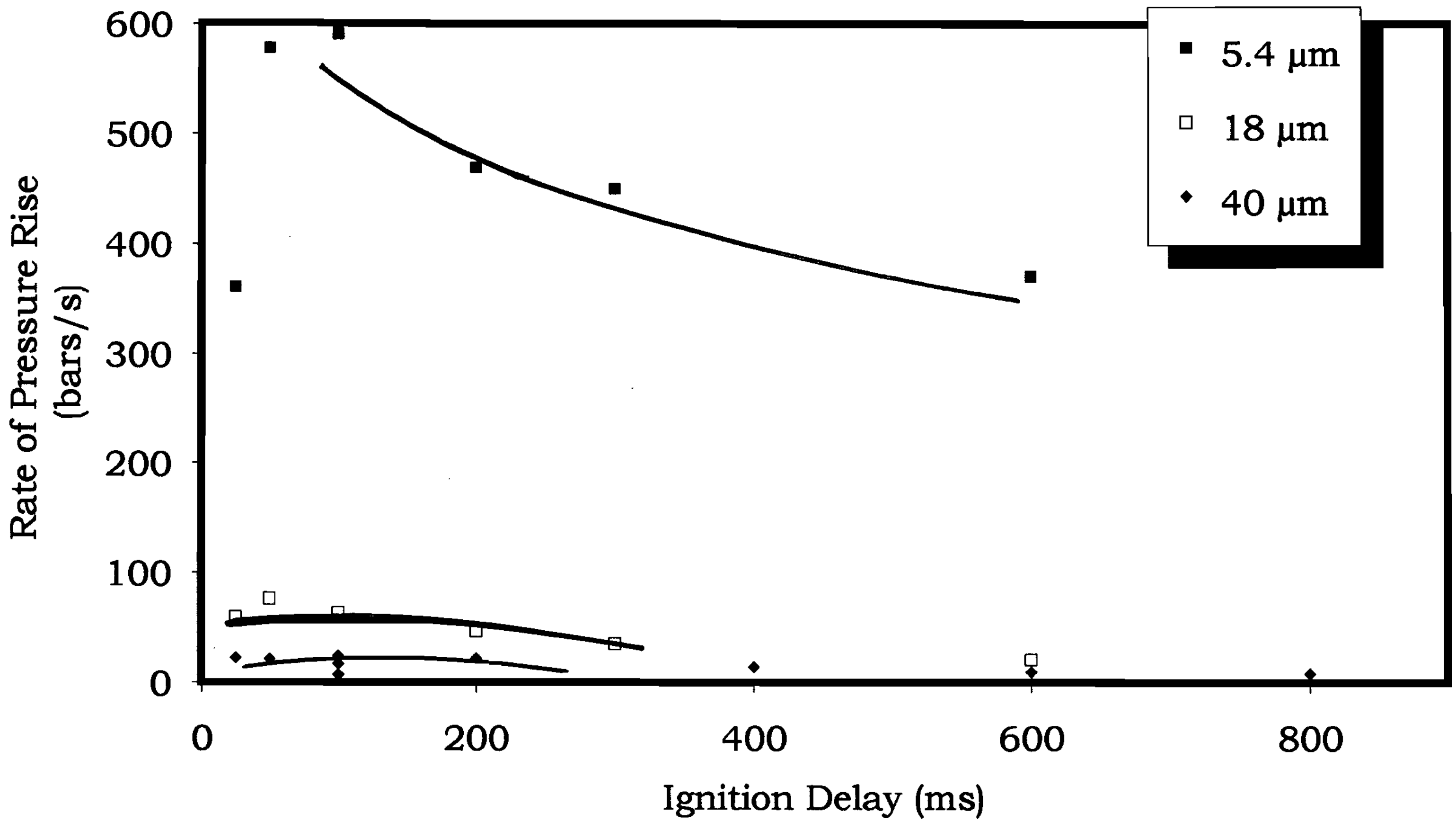

Figure 17: Results of maximum rate of pressure rise using different sizes of aluminum dust particles dispersed using the conical diffuser dispersion system.

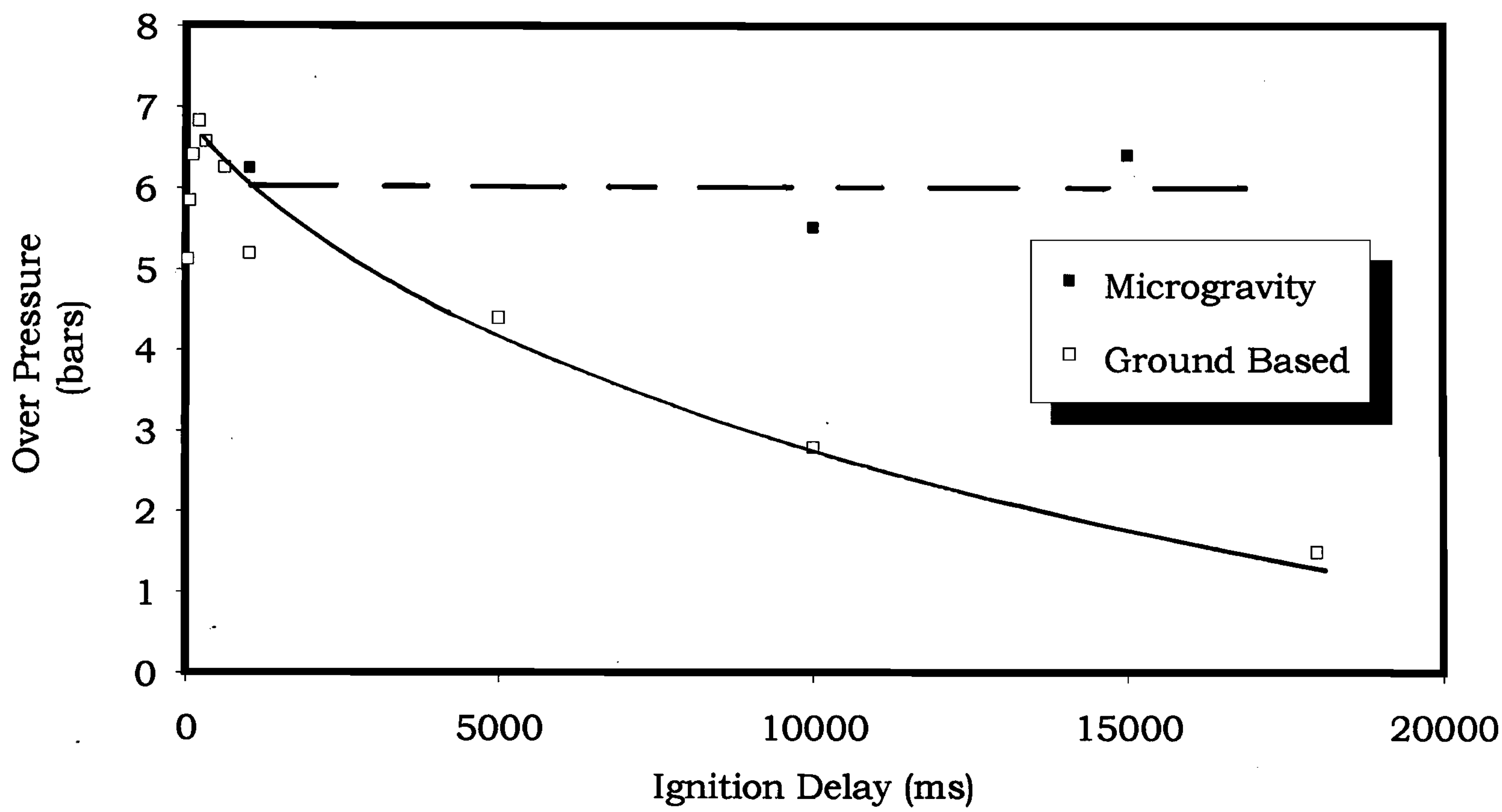

Figure 18: Results of maximum overpressure for experiments performed in microgravity and normal gravity conditions using aluminum dust particles of 5.4 μm dispersed by means of the conical diffuser dispersion system.

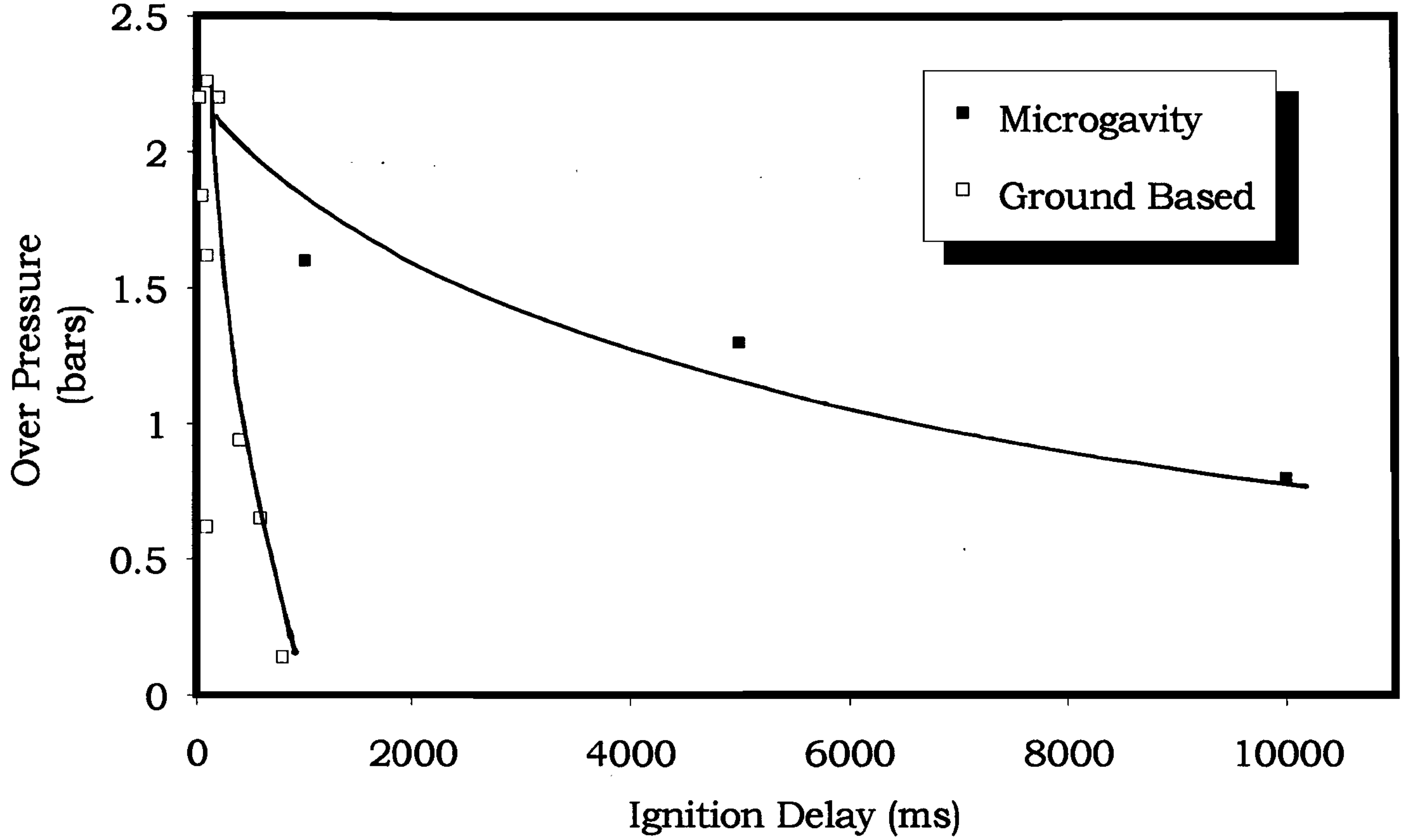

Figure 19: Results of maximum overpressure for experiments performed in microgravity and normal gravity conditions using aluminum dust particles of 40 μm dispersed by means of the conical diffuser dispersion system.

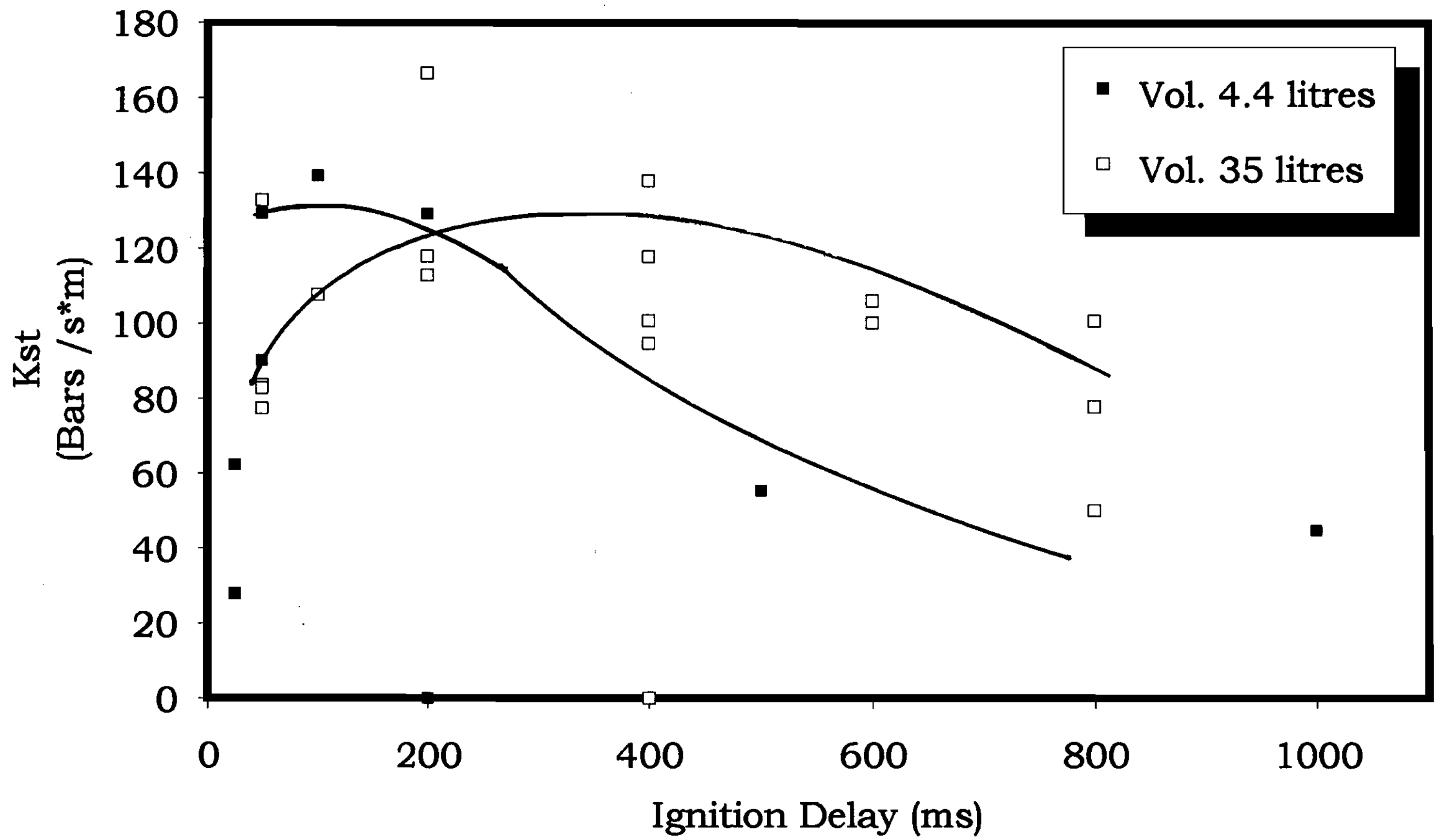

Figure 20: Results of K_{st} for different sizes of combustion chamber using aluminum dust of 5.4 µm dispersed using the Hartmann types dispersion system.

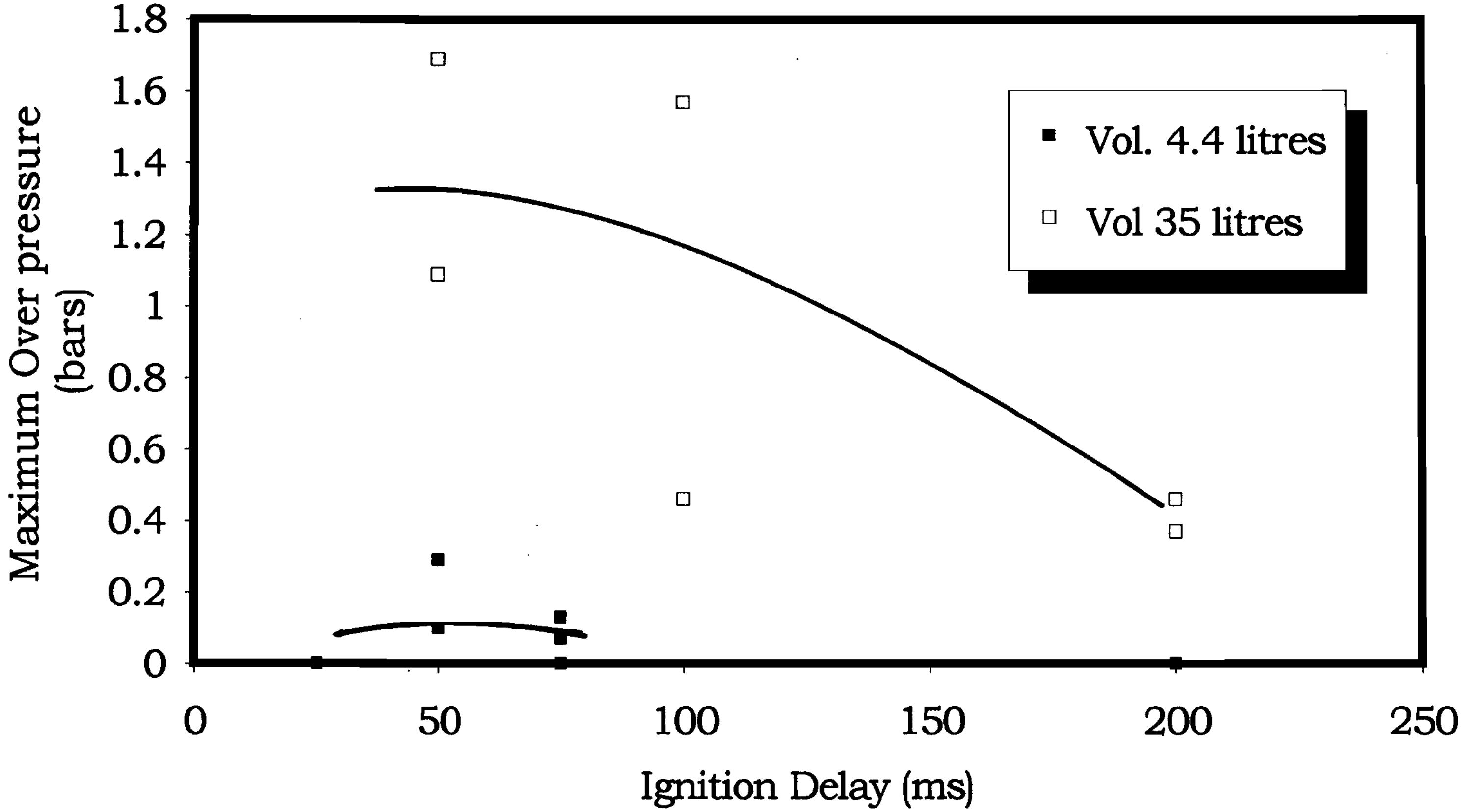

Figure 21: Results of maximum overpressure for different sizes of combustion chamber using aluminum dust of 40 μm dispersed using the Hartmann types dispersion system.

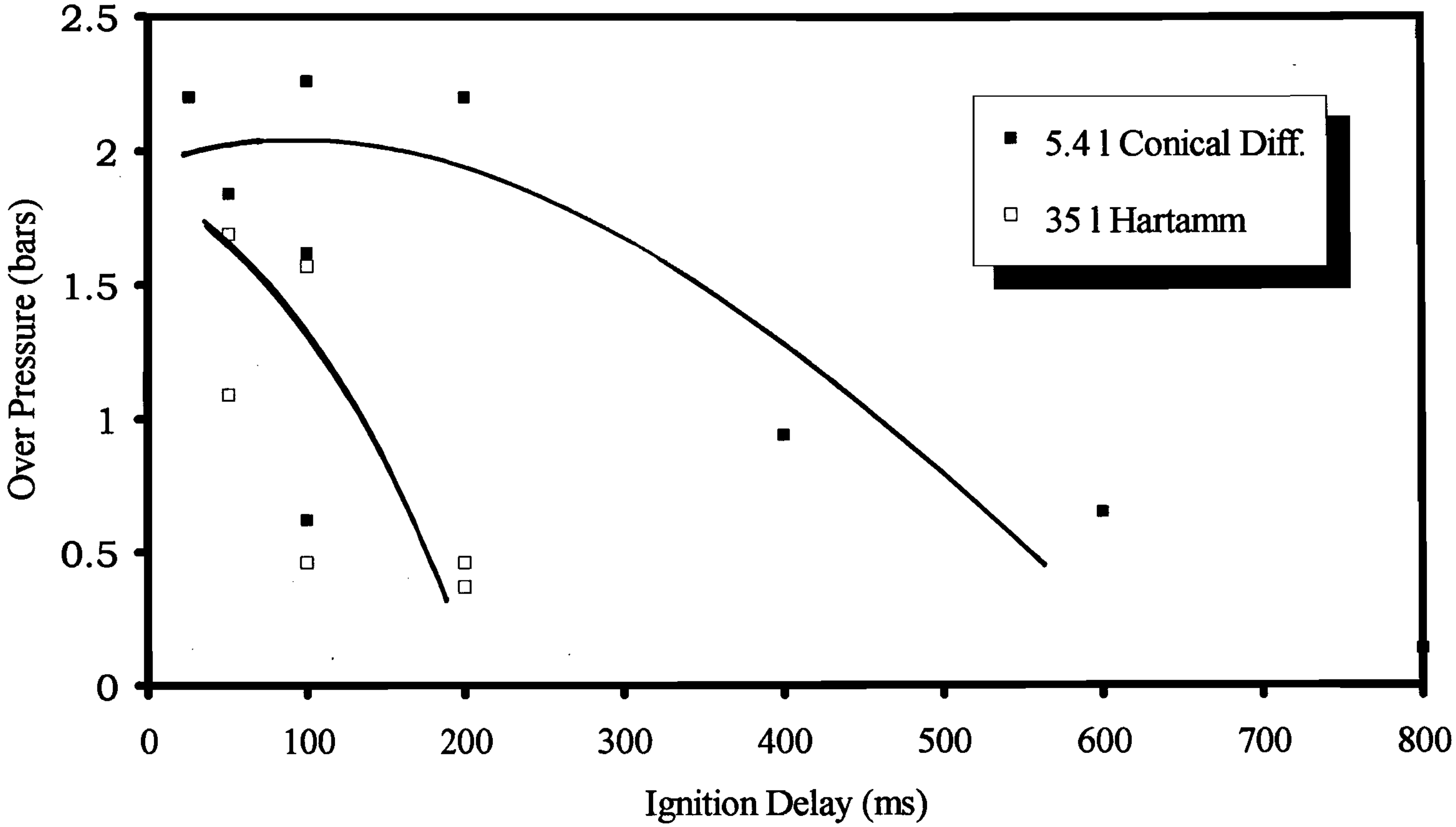

Figure 22: Comparison of the results obtained using the 35 liter vessel equipped with the Hartmann type dispersion system and the 5.4 liter vessel equipped with the conical diffuser.

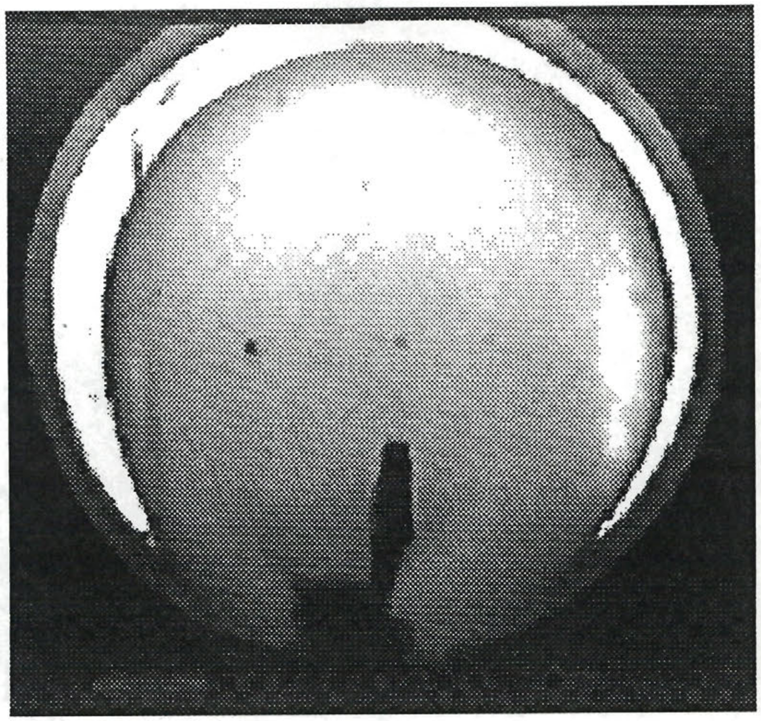

Figure 23: Dispersion of 5.4 μm dust at 0 seconds.

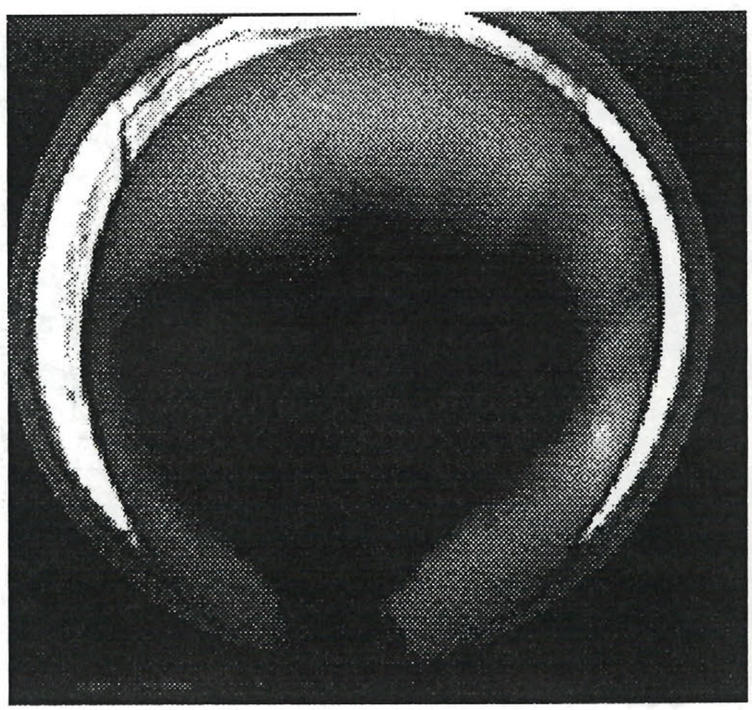

Figure 24: Dispersion of 5.4 μm dust at 0.033 seconds.

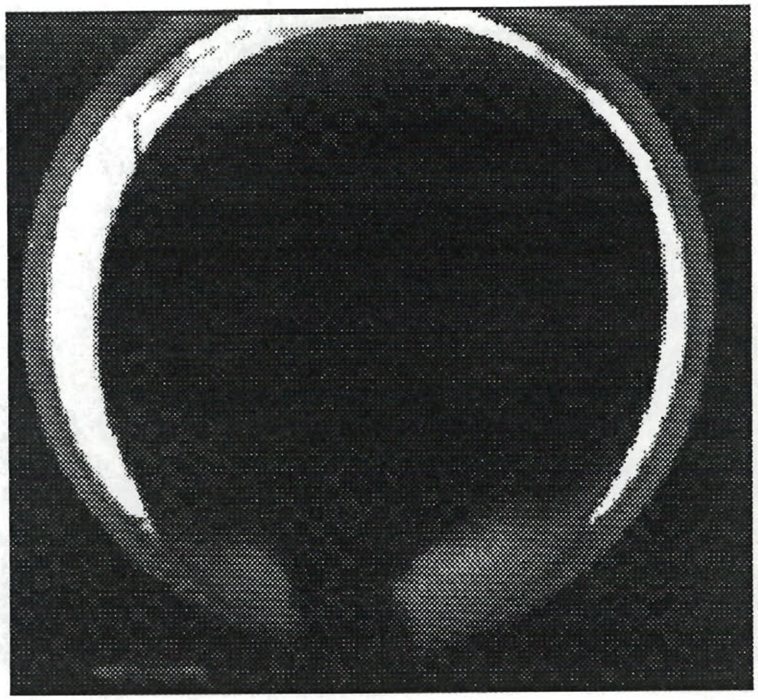

Figure 25: Dispersion of 5.4 μm dust at 0.066 seconds.

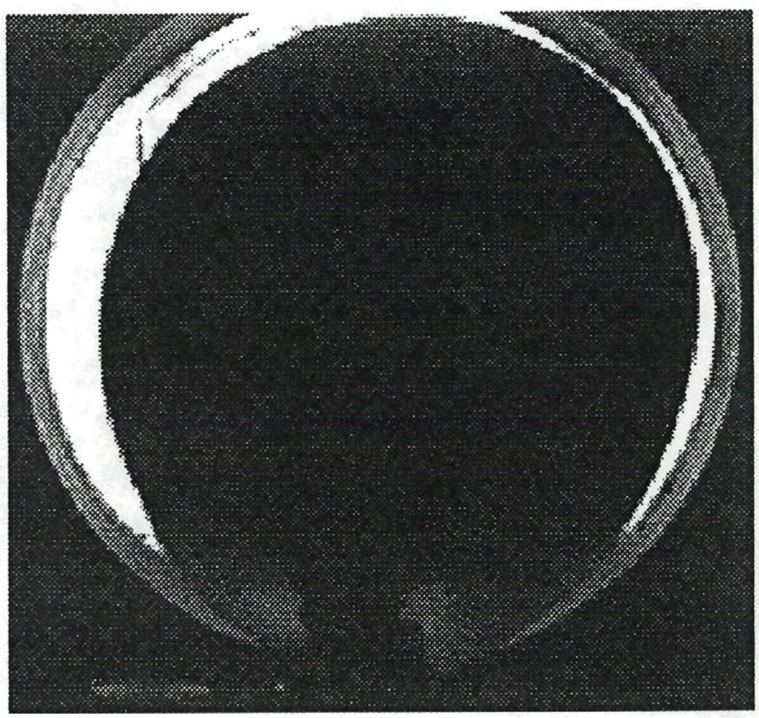

Figure 26: Dispersion of 5.4 μm dust at 0.099 seconds.

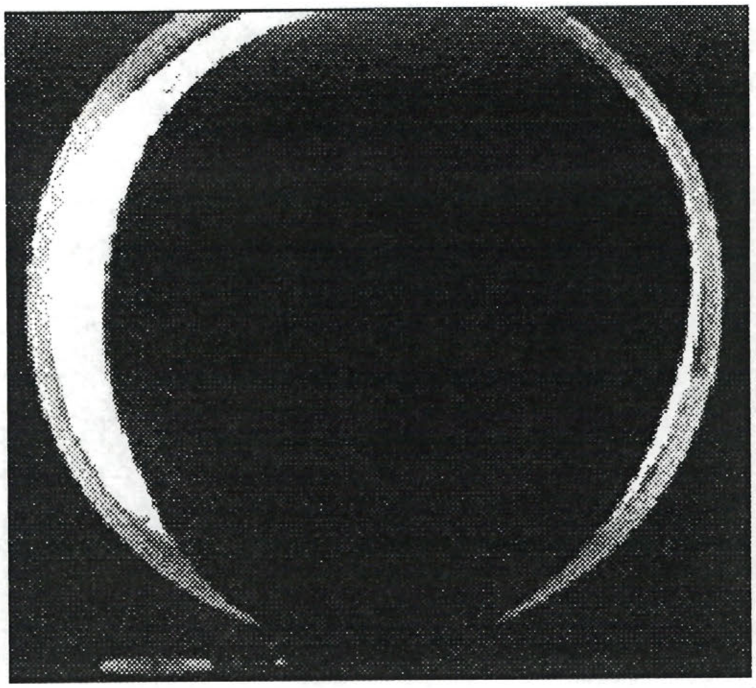

Figure 27: Dispersion of 5.4 μm dust at 0.267 seconds.

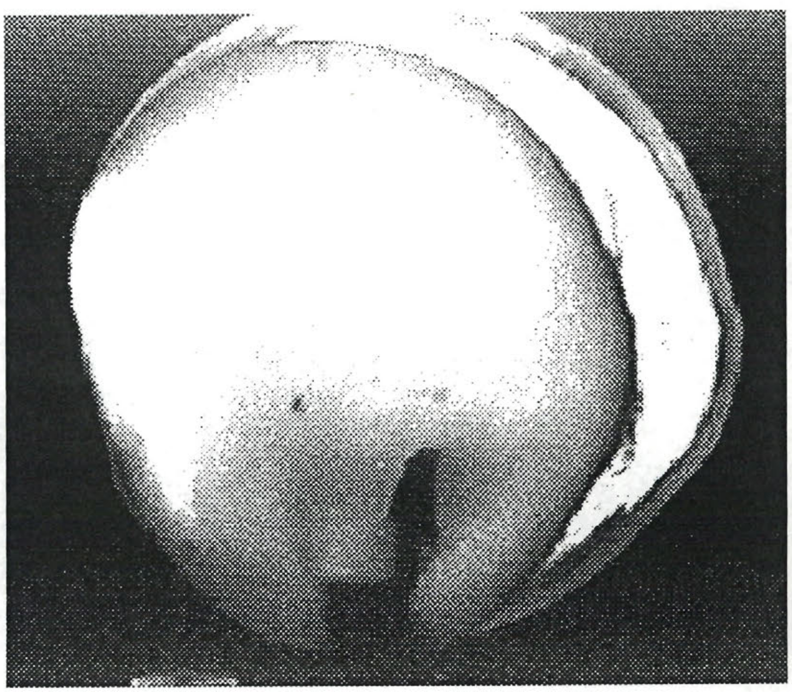

Figure 28: Dispersion of 40 μm dust at 0 seconds.

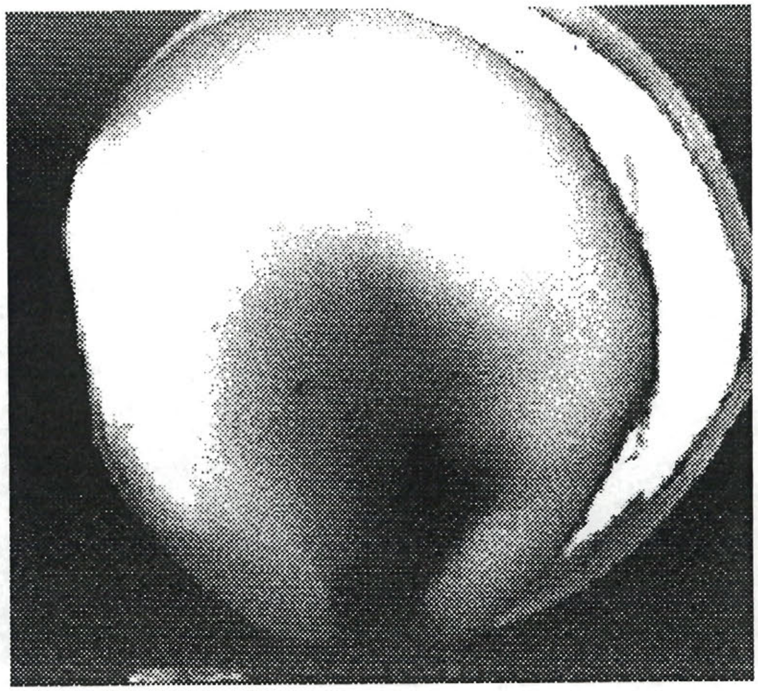

Figure 29: Dispersion of 40 μm dust at 0.033 seconds.

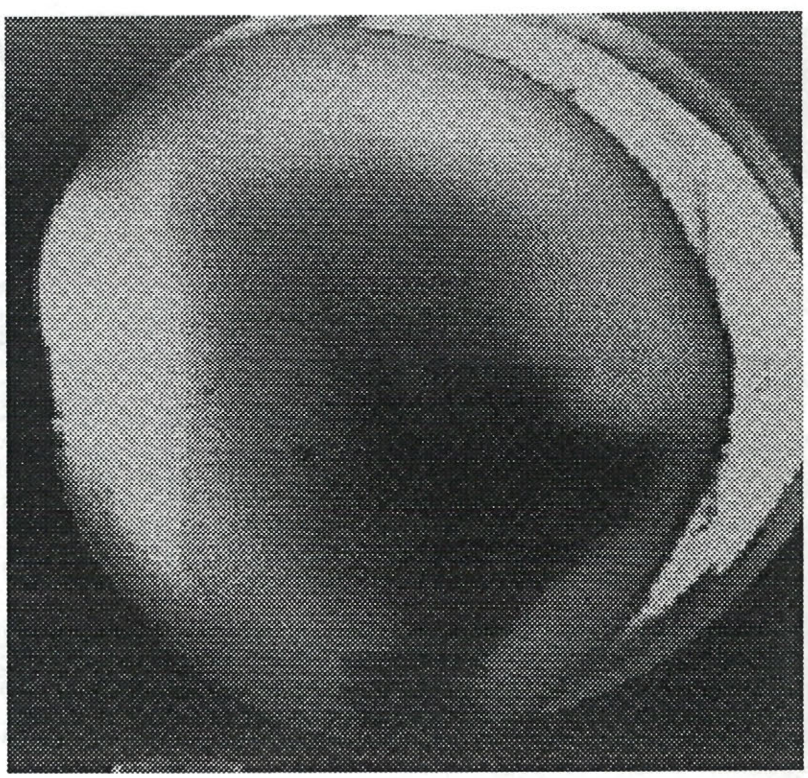

Figure 30: Dispersion of 40 μm dust at 0.066 seconds.

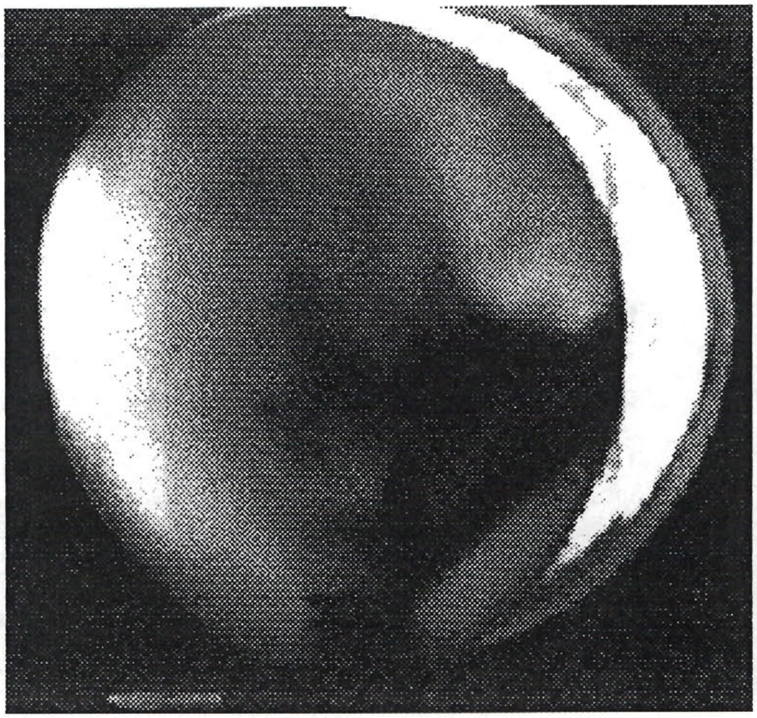

Figure 31: Dispersion of 40 μm dust at 0.099 seconds.

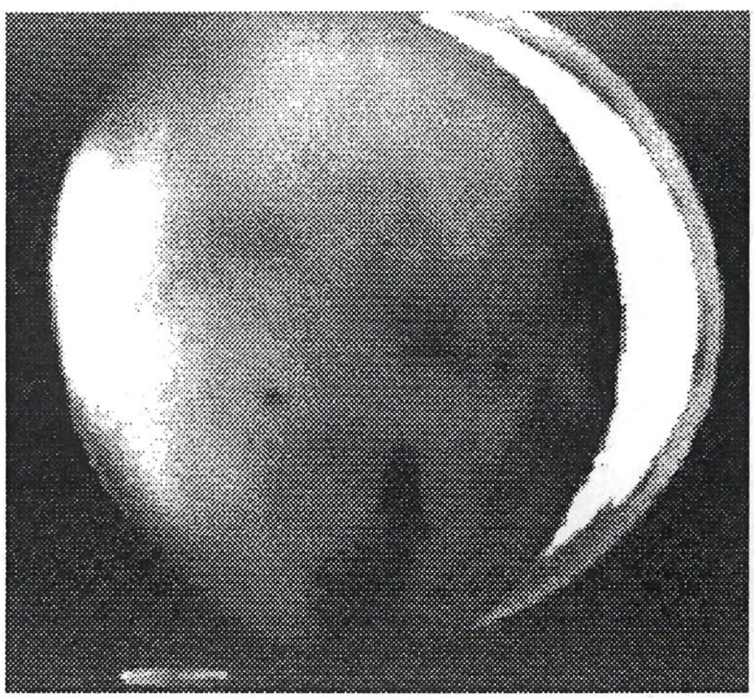

Figure 32: Dispersion of 40 μm dust at 0.267 seconds.

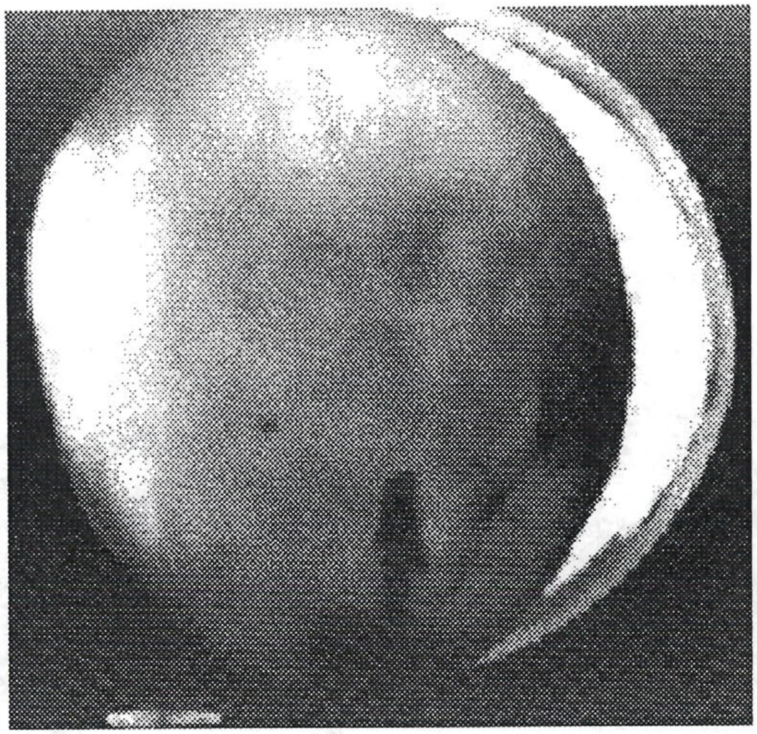

Figure 33: Dispersion of 40 μm dust at 0.33 seconds.

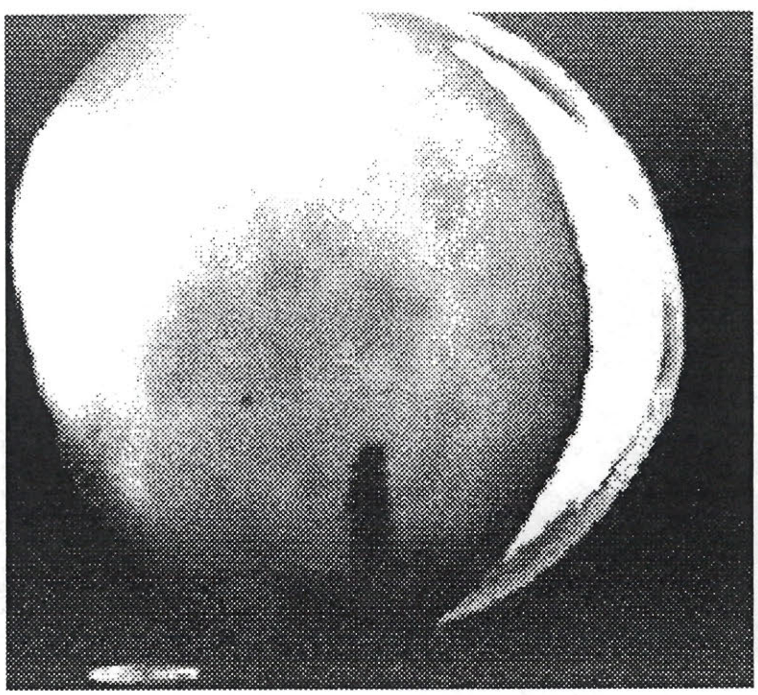

Figure 34: Dispersion of 40 μm dust at 0.5 seconds.